Conjugated Oligoenynes Based on the Diethynylethene Unit

Mogens Brøndsted Nielsen*,† and François Diederich*,‡

Department of Chemistry, University of Copenhagen, Universitetsparken 5, DK-2100 Copenhagen Ø, Denmark, and Laboratorium für Organische Chemie, ETH-Hönggerberg, CH-8093 Zürich, Switzerland

Received October 28, 2004

Contents

* To whom correspondence should be addressed. (M.B.N.) E-mail: mbn@kiku.dk. (F.D.) E-mail: diederich@org.chem.ethz.ch.
† University of Copenhagen.
‡ ETH-Hönggerberg.

1. Introduction

1,2-Diethynylethenes (hex-3-ene-1,5-diynes, DEEs) have found wide interest as potential antitumor agents in medicinal chemistry[1] and as redox active or chromophoric units in advanced materials chemistry.[2] Three constitutional isomers of DEE exist, (*E*)-**1**, (*Z*)-**1**, and *gem*-**1**. These molecules are important synthetic modules, as is the larger tetraethynylethene molecule (3,4-diethynylhex-3-ene-1,5-diyne, TEE, **2**), for construction of conjugated systems in one, two, and three dimensions via acetylenic coupling reactions. Thus, acetylenic scaffolding[3] with suitably functionalized DEEs and TEEs has provided a large selection of extended, carbon-rich chromophores that are formally derived from parent classes of linear and cyclic oligoalkenes, such as the dendralenes, poly(acetylene)s (PAs), radialenes, and annulenes. Carbon-rich macrocycles and cages also play a key role in synthetic endeavors toward buckminsterfullerene, C_{60}.[4] Interest in conjugated oligoenynes has grown because of their potential applications, for example, in molecular wires, switches, and other components for molecular electronics, nonlinear optics (NLO), organic conductors, polyelectrochromic materials, and light-emitting diodes (Chart 1).[5]

The electronic and materials properties of the conjugated scaffolds are strongly dependent on the constituent DEE modules, that is, whether the multiple bonds are linearly conjugated as in (*E*/*Z*)-**1** or cross-conjugated as in *gem*-**1**. Moreover, aryl donor−acceptor functionalization has extensively been employed to tune the properties.[2a] This review covers general synthetic procedures for DEEs and TEEs, their reactivities, and their chromophoric and redox properties in comparison to the extended, linear, or cyclic oligomeric structures.

2. Synthetic Protocols

2.1. Syntheses of (*E*/*Z*)-DEEs

A large selection of methods is available today for the synthesis of (*E*)- and (*Z*)-DEEs. We shall briefly

10.1021/cr9903353 CCC: $53.50
Published on Web 04/21/2005

Mogens Brøndsted Nielsen, born in 1972 in Grenå, Denmark, received his Ph.D. degree in 1999 from the University of Southern Denmark in Odense under the supervision of Professor Jan Becher. During his Ph.D. studies, he spent one year in Professor Fraser Stoddart's group at the University of California in Los Angeles (UCLA). Following postdoctoral studies under Professor François Diederich at ETH in Zürich from 2000 to 2002, he returned to the University of Southern Denmark first as Assistant Professor and in September 2003 as Associate Professor. In February 2004, he moved to a position as Associate Professor at the University of Copenhagen. His research is currently focused on acetylenic scaffolding with dithiafulvenes and tetrathiafulvalenes, targeting new redox active chromophores. He has been awarded the 2004 Knud Lind Larsen prize for his contributions to synthetic and supramolecular chemistry.

François Diederich, born in the Grand-Duchy of Luxemburg (1952), studied chemistry at the University of Heidelberg (1971–1977). He joined the group of Prof. Heinz A. Staab for his diploma and doctoral thesis, which he completed in 1979 with the synthesis of kekulene. Following postdoctoral studies with Prof. Orville L. Chapman at UCLA (1979–1981), investigating arynes in argon matrixes, he returned to Heidelberg for his Habilitation at the Max-Planck-Institut für Medizinische Forschung (1981–1985). Subsequently, he joined the Faculty in the Department of Chemistry and Biochemistry at UCLA where he moved up the ranks to become Full Professor of Organic and Bioorganic Chemistry in 1989. In 1992, he returned to Europe, joining the Laboratory of Organic Chemistry at the ETH Zürich. His research interests, documented in more than 450 publications, span from medicinal chemistry, with a focus on molecular recognition studies, to dendritic mimics of globular proteins, and to advanced fullerene and acetylene-based materials with novel optoelectronic properties.

go through those depicted in Scheme 1. Treatment of tosylate **3** with an excess of 1,5-diazabicyclo[4.3.0]-non-5-ene (DBN) in diethyl ether at room temperature leads to the formation of (*E*/*Z*)-**1** (70% yield) via elimination in a ratio of ca. 3:2 (route a).[6] Solution pyrolysis of *cis*-1,2-diethynylthiirane **4** (or the trans isomer) in toluene (100 °C) results in desulfurized products with greater than 90% retention of configuration (route b).[7] Alternatively, zinc reduction of

Chart 1

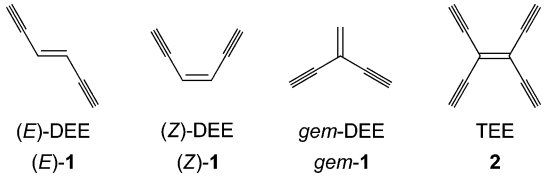

Scheme 1. Synthesis of (*E*)- and (*Z*)-DEEs[a]

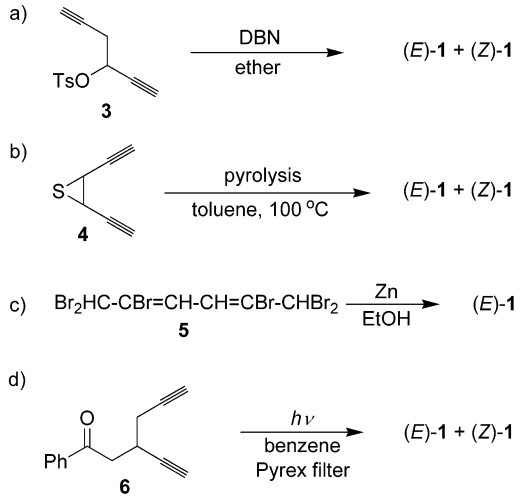

[a] Ts = *p*-toluenesulfonyl.[6–9]

hexabromide **5** affords (*E*)-**1** in 57% yield (route c).[8] Photolysis of 3-(2-phenyl-2-oxoethyl)hexa-1,5-diynes provides another route (d).[9] Accordingly, irradiation of **6** provides enediynes (*E*/*Z*)-**1** as a 1:1 mixture in a yield of 45%. Thermal decomposition of 1,4-diiodobenzene **7** in a reactor (at 960 °C) coupled to a mass spectrometer revealed the formation of the 1,4-benzene diradical (**8**) that can undergo reverse Bergman cyclization (vide infra) (Scheme 2).[10]

Scheme 2. Thermal Decomposition of 1,4-Diiodobenzene[10]

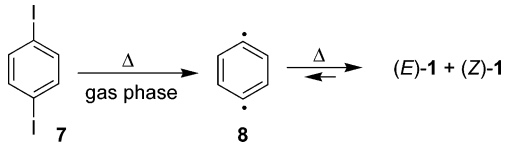

Photolysis (route d, Scheme 1) of diethynylethanes (**6**) susbtituted with methoxymethyl groups at the alkynyl positions affords substituted DEEs in extremely high yield (95%).[9] Other methods for the synthesis of substituted DEEs are provided in Scheme 3. Metal-catalyzed cross-coupling between alkenyl halides (**9** or **10**) and terminal acetylenes or metal acetylides provides one of the most versatile routes for enediynes of general structure (*E*/*Z*)-**11** (route a).[11] The stereochemical outcome of the reaction is higly dependent on the experimental conditions and the substituents on the alkene groups. A variety of DEEs were synthesized by Jones and co-workers[12] from precursor **12** via a carbenoid coupling−elimination strategy (route b), which was tolerant of a wide range of functionalities. Reaction parameters can be adjusted to control the stereoselectivity from 1:12 to >100:1 *E*:*Z* ratios. The preparation of DEEs via sequential acetylide reductive coupling and alkyne

Scheme 3. Synthesis of Substituted (*E*/*Z*)-DEEs[a]

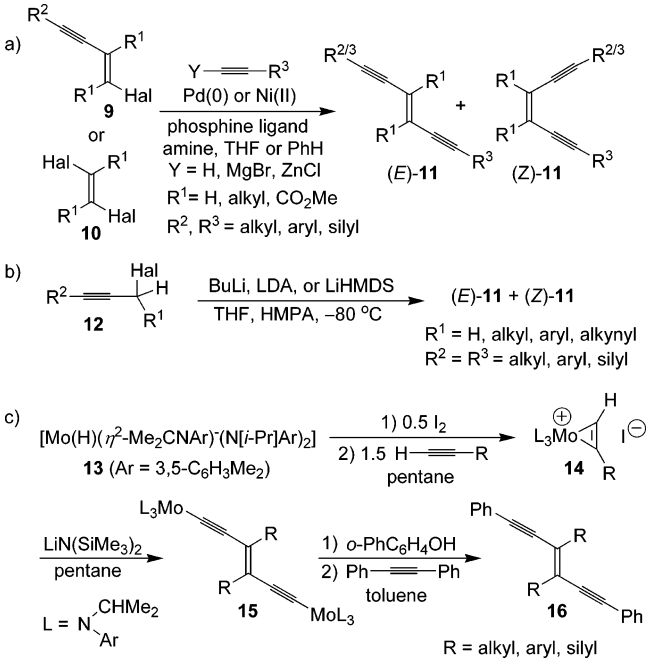

[a] LDA = lithium diisopropylamide; HMDS = hexamethyldisilazane; and HMPA = hexamethylphosphorus triamide. The Ni(II) catalyst corresponds to $[Cl_2Ni(Ph_2P(CH_2)_3PPh_2]$. The Pd(0) catalyst system corresponds to $[PdCl_2(PPh_3)_2]$/CuI or $[Pd(PPh_3)_4]$/CuI.[11–13]

metathesis is presented in route c.[13] From the molybdaziridine hydride **13**, molybdenum(VI) alkyne complexes **14** were prepared in high yield and subsequently converted to the dinuclear enedialkylidyne complexes **15** upon deprotonation. Replacement of the electron-rich amido ligands with 2-phenylphenoxy ligands followed by treatment with diphenylacetylene finally provided the DEEs of general structure **16**. A related protocol allows the synthesis of cycloalkenediynes.

Moreover, Yamamoto and co-workers[14] devised a method for converting diynes such as **17** to (*E*)-1,2-divinyl-1,2-diethynylethene derivatives **18** (Scheme 4). The reaction proceeds via a Pd-catalyzed dimerization. Yields between 40 and 82% were obtained.

Scheme 4. Synthesis of (*E*)-1,2-Divinyl-DEEs[14]

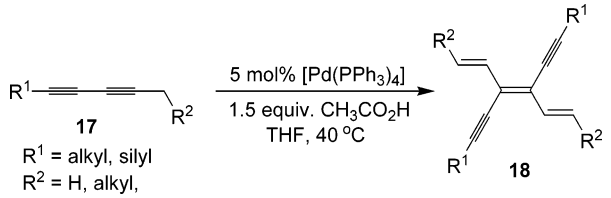

2.2. Synthesis of *gem*-DEEs

The first method for the preparation of *gem*-**1** was reported by Böhm-Gössl et al.[15] in 1963 (Scheme 5). It was based on nucleophilic carbonyl addition followed by elimination of H_2O. Thus, addition of either methylmagnesium bromide to **19** or acetylide magnesium bromide to **20** affords the tertiary alcohol **21** that subsequently eliminates H_2O upon treatment with *meta*-phosphoric acid.

In a similar nucleophilic addition–elimination procedure, *gem*-DEEs with substituents at the

Scheme 5. Synthesis of the Parent *gem*-DEE[15]

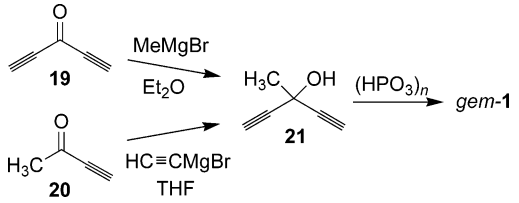

alkynyl positions can be prepared from terminal lithium acetylides (Scheme 6, route a). Upon double

Scheme 6. Synthesis of Substituted *gem*-DEEs[a]

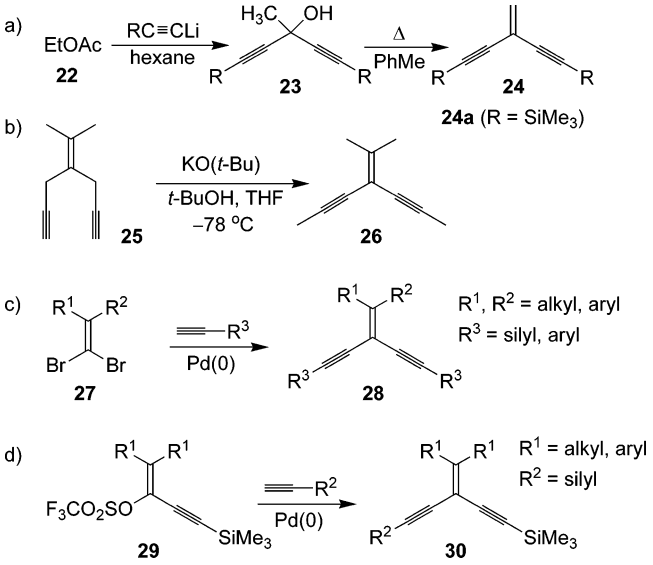

[a] The Pd(0) catalyst system corresponds to $[PdCl_2(PPh_3)_2]$/CuI or $[Pd(PPh_3)_4]$/CuI.[16–19]

addition to ethyl acetate (**22**), product **23** is formed. This compound loses H_2O upon heating, resulting in *gem*-DEE **24**.[16] *gem*-DEEs with substituents at both the ethynyl and the ethenyl positions can be prepared by routes b–d (Scheme 6). Gleiter et al.[17] found that a base-promoted rearrangement of diyne **25** afforded **26** (route b). Polymeric byproducts were formed as well. Pd-catalyzed cross-coupling between vinylic dihalides of general structure **27** and terminal acetylenes presents an efficient route (c) to substituted *gem*-DEEs of the general structure **28**.[18] Pd-catalyzed alkynyl cross-coupling of vinyl triflates (**29**) provides

Scheme 7. Synthesis of Tri- and Tetraethynylethenes[21–23]

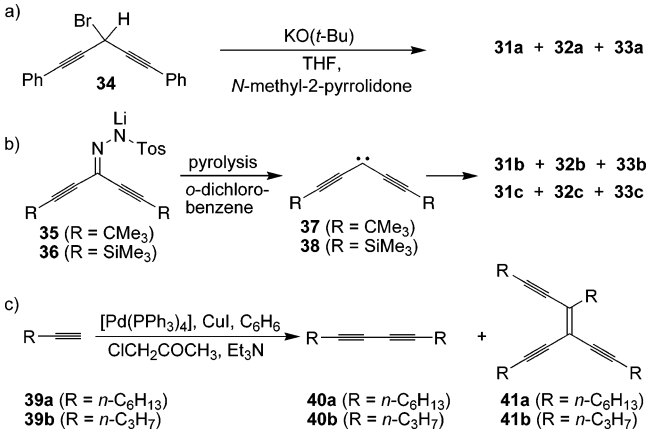

Chart 2

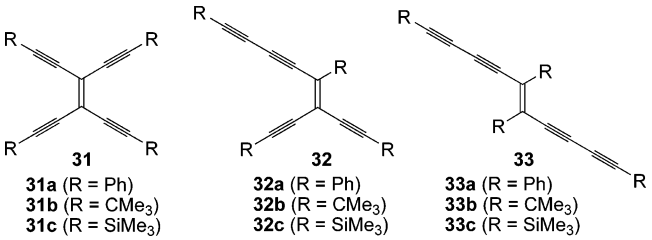

a versatile method to obtain a variety of unsymmetrically substituted *gem*-DEEs (**30**) (route d).[19] This reaction does not work when $R^1 = H$. As a final comment to the synthesis of *gem*-DEEs, we note that 1,1-diethynylallenes also have been reported in the literature.[20]

2.3. Synthesis of Tri- and Tetraethynylethenes

Tetrakis(phenylethynyl)ethene **31a** was the first tetraethynylethene derivative synthesized by Hori et al.[21] in 1969. A mixture of three compounds, **31a**, **32a**, and **33a**, are formed upon treatment of 3-bromo-1,5-diphenylpenta-1,4-diyne **34** with potassium *tert*-butoxide (Scheme 7, route a). A few years later, Hauptmann[22] prepared the first peralkylated and persilylated derivatives **31b**,**c**, **32b**,**c**, and **33b**,**c** by pyrolysis of the lithium salts of diethynyl ketone tosylhydrazones **35** and **36** (route b). This reaction proceeds via dimerization of intermediate diethynylcarbenes **37** and **38**. Route c provides a method for the preparation of enetriynes. Thus, reaction of terminal alkynes **39a**,**b** with a solution of chloroacetone and Et_3N in benzene, in the presence of [Pd(PPh_3)$_4$] and CuI, affords buta-1,3-diynes **40a**,**b** together with triethynylethenes **41a**,**b** (Chart 2).[23]

Other synthetic routes to TEEs with four identical substituents are depicted in Scheme 8. The first two routes proceed via elimination reactions of 1,1,2,2-tetraethynylethane derivatives, either by base-induced elimination (substrate **42**, route a)[24] or by acid-catalyzed thermal elimination of an ortho ester (substrate **43**, route b).[25] Recently, Low and co-workers[26] constructed the TEE core by a Pd(0)-catalyzed 4-fold cross-coupling reaction between tetrachloroethene **44** and terminal acetylenes (route c).

Diederich and co-workers[27,28] introduced in the early 1990s more general protocols that took advantage of Pd(0)-catalyzed cross-coupling reactions of 1,1-dibromo-2,2-diethynylethenes **46** for the synthesis of geminally substituted TEEs of general formula **47** (Scheme 9). Triethynylethenes have been prepared in a similar way from suitable dibromides.[29] The sequence **48** → **49** → **50** (Scheme 9) provides an efficient route to trans-substituted TEEs. These methods that allow access to virtually any desired substitution pattern have been comprehensively reviewed.[28] 1,1-Dibromo-2,2-diethynylethenes serve as useful precursors for other conjugated systems as well. Thus, triynes are generated upon treatment with BuLi via alkyne migration in the intermediate carbene/carbenoid species.[30] Finally, it should be mentioned that the carbenoid coupling−elimination strategy introduced by Jones and co-workers[12] for enediynes also allows preparation of TEEs from suitable precursors.

Scheme 8. Synthesis of TEEs[a]

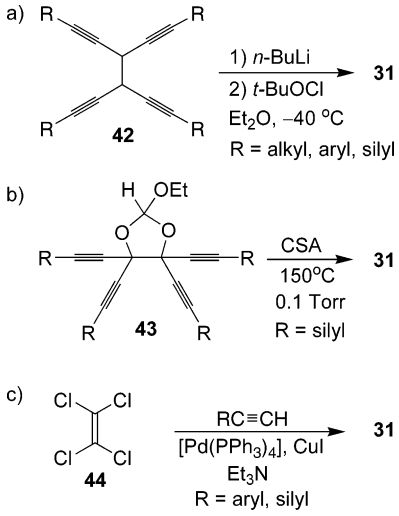

[a] CSA = camphorsulfonic acid.[24−26]

3. Chemistry of DEEs

3.1. Reactions of (*E*/*Z*)-DEEs

(*E*)- and (*Z*)-DEEs are in thermal equilibrium. However, the rotational activation enthalpy ($\Delta H^{\ddagger}$) is very high and was determined by Roth et al.[31] to be 48.1 kcal mol^{-1}. At elevated temperature (typically higher than 180 °C), (*Z*)-DEE undergoes Bergman cyclization,[32] which leads to the aromatic 1,4-diradical system **8** (Scheme 10, route a). This diradical can be trapped in the gas phase with O_2 or NO, and from the kinetics of these trapping reactions, the heat of

Scheme 9. Synthesis of Unsymmetrical TEEs[a]

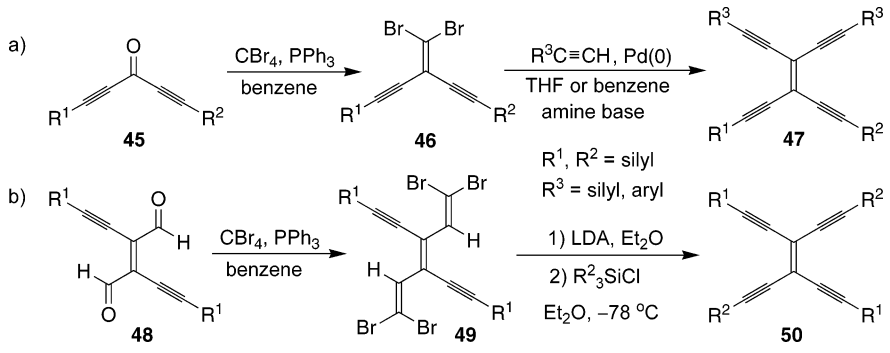

[a] LDA = lithium diisopropylamide.[27,28]

Scheme 10. Reactions of (*E*/*Z*)-DEEs[6,32,38,40a]

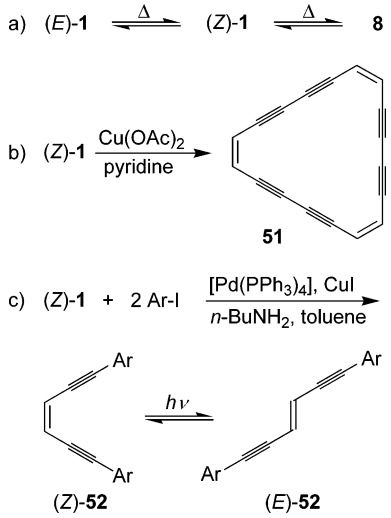

formation of **8** was determined to be 138 ± 1 kcal mol^{-1} [8.5 kcal mol^{-1} less stable than (*Z*)-**1**], and the barrier toward ring opening was determined to be 19.8 kcal mol^{-1}.[33] The Bergman cyclization, also referred to as cycloaromatization, is responsible for the biological activities of enediynes, since the diradical is able to cleave DNA. Natural products undergo Bergman cyclization under ambient conditions after being activated by a triggering reaction.[34] Photochemical Bergman cyclization reactions have been reported to occur at room temperature but usually require specific substitution of the alkynes (alkyl or aryl).[35]

The terminal acetylene moieties of (*E*/*Z*)-DEEs can be subjected to various metal-catalyzed C−C coupling reactions.[36] One example involves oxidative Glaser−Eglinton[37] cyclization of (*Z*)-**1** to afford the dodecadehydro-[18]annulene **51** (route b).[6,38] The [18]annulene is exclusively obtained in this cyclization; that is, higher cyclic oligomers are absent. Two-fold palladium-catalyzed Sonogashira[39] coupling of various iodoarenes with (*Z*)-**1** at room temperature provides diarylated DEEs of general structure (*Z*)-**52** in yields ranging from 23 to 68% (route c).[40a] In all cases, complete retention of the *Z*-configuration of the enediyne was observed. The products isomerize, however, rapidly when the solutions are exposed to sunlight or irradiated with low intensity UV light at 366 nm.[40a−d] In the case of donor−acceptor-substituted diarylated DEEs, the equilibrium in the photostationary state is strongly affected by both the nature of the aryl substituents and by the solvent polarity.[40b] Electrochemical cis to trans isomerization of donor−acceptor-substituted DEEs has also been described.[40e]

3.2. Reactions of *gem*-DEEs

The reactivity of the parent 3-methylenepenta-1,4-diyne (*gem*-**1**) has never been described. However, Alberts[16] investigated 1,5-bis(trimethylsilyl)-3-methylenepentadiyne **24a** (Scheme 11). This compound can be polymerized without a catalyst in the absence of solvent in an inert atmosphere to a pale yellow solid (0 °C, 4−5 days, 60% yield, MW 4000−

Scheme 11. Polymerization Reaction of *gem*-DEE[16]

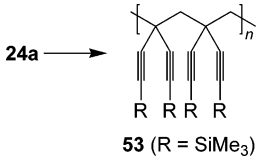

determined by osmometry in $CHCl_3$ and gel permeation) or an ochre-colored solid (80 °C, 30 min, 40% yield, MW 14000). The structure **53** was proposed for these polymers resulting presumably from a selective polymerization of the double bonds in **24a**.[41]

gem-DEEs can also undergo oxidative Glaser couplings[42] as well as Sonogashira couplings. They cannot, however, follow the Bergman cyclization pathway since five carbon atoms are involved with only five π-electrons. However, the missing electron can be supplied by reduction as elegantly demonstrated by Eshdat et al.[43] Upon reduction of the fluorene derivative **54** with potassium in vacuo at 258 K in an extended NMR tube, the formal Bergman cycloaromatization product **55** forms (Scheme 12), that is, a pentafulvene dianion.

Scheme 12. Bergman Cycloaromatization of *gem*-DEE Induced by Electron Uptake[43]

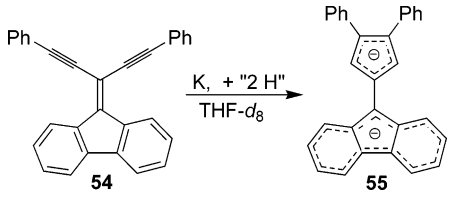

Finally, we note that Neckers and co-workers[18c,44] have demonstrated that arylated *gem*-DEEs are able to undergo a similar photochemical cyclization that converts arylated enynes into fused benzene rings.[45]

3.3. Bergman Cyclization of Cyclic Enynes

Much attention has been focused on enediyne antitumor agents, which, after suitable activation steps, undergo Bergman cyclization to yield a 1,4-diradical, capable of generating oxidative lesions on DNA leading ultimately to strand scission and cell death. These molecules contain enediyne moieties in a cyclic framework and include the calicheamicins,[46] esperamicins,[47] neocarzinostatin chromophores,[48] kedarcidin,[49] C-1027 chromophore,[50] and dynemicin.[51]

The possibility for Bergman cyclization of other cyclic enynes has attracted the interest of several groups. Thus, Behr et al.[52] investigated possible cycloaromatization reactions of compound **56** long before the Bergman reaction had been recognized (Scheme 13). Compound **56** does, however, not undergo Bergman cyclization, presumably due to the strain that would develop in the transition state. However, an attempt to hydrogenate the four triple bonds gave the expected tricyclic product in only 50%, whereas the product **57** of transannular bond formation was formed in 40%. In addition, Pilling and Sondheimer[53] observed a similar reaction upon hydrogenation of **58**, affording **59**.

Scheme 13. Unexpected Products of Hydrogenation[52,53]

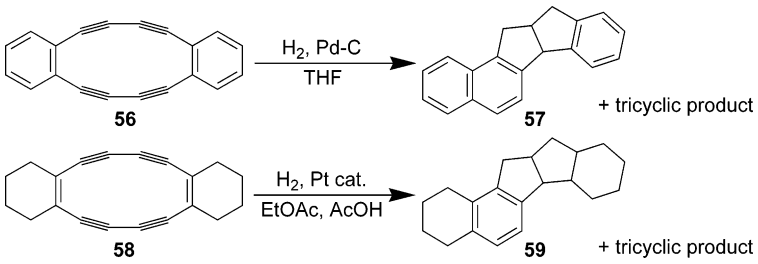

Schreiber and co-workers[54] have investigated the ability of cyclic enetetraynes to undergo Bergman cyclization. The macrocycles **60** and **61** were individually heated in benzene in the presence of 1,4-cyclohexadiene, but no cyclization occurred; only starting material and an insoluble solid could be recovered from the reaction mixture. The *cis*-DEE dimer-containing macrocycle **62** was subjected to the same conditions, which again only resulted in insoluble decomposition products. Enhanced strain in the transition state was suggested based on calculations to account for the lack of reactivity. Thermolysis of the acyclic *cis*-DEE dimer **63** revealed the formation of biphenyl, the product of two Bergman reactions, albeit in low yield. Numerous other products had incorporated one or more cyclohexadienes into biphenyl type structures (Chart 3).

Chart 3

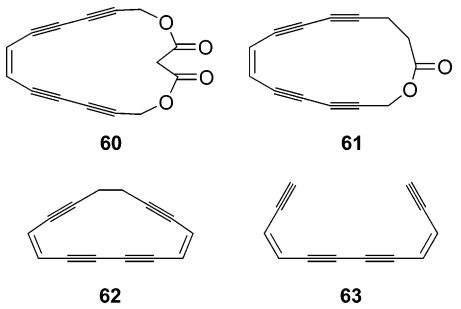

3.4. Reactions of TEEs

In contrast to enediynes, TEEs do not undergo the Bergman cyclization. Other decomposition channels presumably become dominant. One of the striking characteristics of TEE derivatives is the complete chemical inertness of the central olefinic bond.[55] All attempts to add electrophiles, carbenes, 1,3-dienes, or 1,3-dipoles to this electron deficient bond have failed.[56] Thus, 1,3-dipolar cycloaddition with diazomethane took place at one of the terminal C≡C bonds rather than at the central C=C bond. Similarly, oxidations or epoxidations of this bond were unsuccessful.

The stability of TEEs (as well as of DEEs) largely depends on the number of free ethynyl residues in the molecule.[57] If all acetylene residues are silylated, alkylated, or arylated, the compounds are kinetically very stable and display high melting points or decomposition points, which, in the case of arylated derivatives, reach 200 °C and higher. When the number of free terminal alkyne groups is increased, the stability rapidly decreases; derivatives with two ethynyl residues already are quite labile in the neat state, and the parent TEE rapidly decomposes at 25 °C.

The unique TEE framework facilitates π-conjugation with pendant aromatic substituents by allowing coplanar orientation throughout the molecular core, as first demonstrated in the X-ray crystal structure of tetrakis(phenylethynyl)ethene **31a** by Hopf and coworkers.[58] In contrast, coplanarity is prevented by steric interactions in molecules such as *cis*-stilbenes or tetraphenylethene.[59] As a result of strain-free planarity, cis- and trans-arylated TEEs are bistable states that interconvert upon photochemical excitation without competition from undesirable thermal isomerization.[40b] This photoisomerization is not exhibited by the nonarylated derivatives.[60] The trans to cis isomerization is of preparative use for the synthesis of *cis*-TEEs that are otherwise difficult to obtain. For example, (*E*)-**64** is partly converted to its (*Z*)-isomer by irradiation at 366 nm (Scheme 14).

3.5. Molecular Switches Based on TEE

The TEE isomerization process has been employed for the construction of light-driven molecular switches.[61] The complex, highly programmed system (*E*)-**65a** (Scheme 15) was constructed, which combines the *Z*/*E*-isomerizable TEE unit with two other addressable subunits, a photoswitchable dihydroazulene (DHA)/vinylheptafulvene (VHF) moiety and a proton sensitive dimethylaniline (DMA) group.[61a,c] This three-way chromophoric molecular switch is in principle able to carry out individual, reversible switching cycles between as much as eight states. DHA derivatives are known to undergo, after light irradiation, a

Scheme 14. Light-Induced trans → cis Isomerization of Arylated TEE[40b]

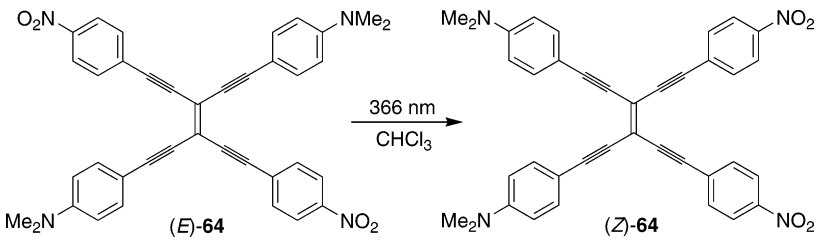

Scheme 15. Three-Way Chromophoric Molecular Switch[61a,c]

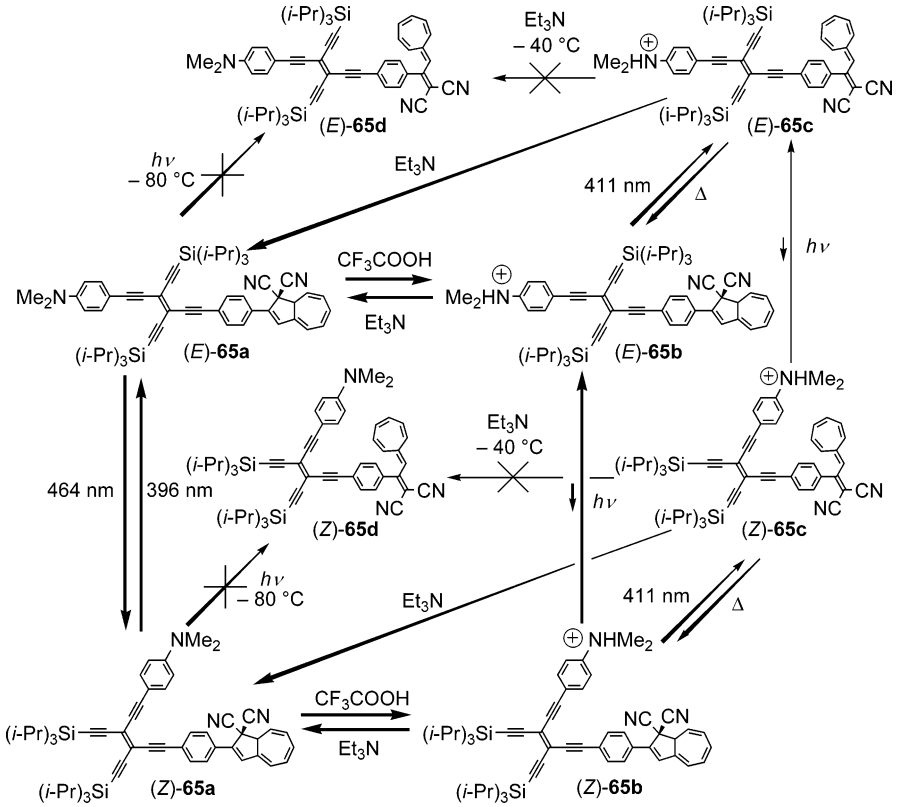

10-electron retro-electrocyclization to the isomeric VHF compounds,[62] which, in turn, undergo a thermal cyclization back to the DHA forms. However, when incorporated into the TEE derivative (*E*)-**65a**, this switching capacity of the DHA chromophore is altered. Thus, irradiation of (*E*)-**65a** caused reversible *E*−*Z* isomerization of the TEE core only, leaving the DHA moiety unchanged. Yet, protonation of the third subunit, the DMA substituent, brings about the DHA→VHF photoreaction. Thus, irradiation of the protonated species (*E*)-**65b** results in retro-electrocyclization to (*E*)-**65c** that is able to thermally cyclize back to (*E*)-**65b**. Clean isosbestic points in the UV/vis spectra imply that only this DHF/VHF equilibrium is taking place, which is explained by the fact that the TEE *E*−*Z* isomerization process is much slower. It was not possible to prepare (*E*)-**65d** upon deprotonation of (*E*)-**65c** by triethylamine, since this reaction was accompanied by retro-electrocyclization to (*E*)-**65a**. Thus, the nonprotonated VHF-containing conjugate (*E*)-**65d** [as well as the VHF isomer (*Z*)-**65d**] cannot be obtained in the three-dimensional switching diagram. Consequently, out of the eight potential states of **65**, six are accessible and can be individually addressed by the various switching modes.

The failure of photochemical DHA→VHF isomerization in (*E*)-**65a** was explained in a joint experimental and computational study by Lüthi and coworkers.[63] The neutral conjugate exhibits a strong fluorescence emission that almost completely disappeared after protonation to (*E*)-**65b**. The maximum of this intense emission was found to be strongly dependent on solvent polarity, and in hexane, a dual fluorescence (λ_{max} = 505 and 541 nm; λ_{exc} = 420 nm) was observed. In more polar solvents, such as CH_2Cl_2, the emission spectrum featured only a single, strongly red-shifted band (λ_{max} = 602 nm). Time-dependent density functional calculations on the excited state of related DMA-substituted TEEs suggested that the DHA→VHF isomerization channel is quenched in (*E*)-**65a** by an efficient relaxation of the vertically excited singlet state to an emitting twisted intramolecular charge transfer (TICT) state.[64] This suggestion would account for the experimentally observed dual fluorescence. In the lower energy TICT state, either the dimethylamino group is twisted into an orthogonal position with respect to the planar arylated TEE moiety or the entire DMA group takes an orthogonal orientation with respect to the TEE moiety. The calculations suggested that the twist of the dimethylamino group is the more probable one.

4. Electronic and Structural Properties

4.1. Di-, Tri-, and Tetraethynylethenes

The lowest energy absorption maxima for simple DEEs, triethynylethenes, and tetraethynylethenes are listed in Table 1.[6,11a,16,22,23,27b,65,66] First, we notice that (*E*)- and (*Z*)-DEEs exhibit similar absorption maxima, e.g., by comparison of (*E*)-**1** and (*Z*)-**1** or (*E*)-**66** and (*Z*)-**66**. A red shift is observed when the substituents R are changed from H (**1**) to $SiMe_3$ (**66**). Less efficient π-electron delocalization via cross-conjugation than via linear conjugation is revealed by comparing (*E*)-**67** and **69** or (*E*/*Z*)-**66** and **24a**. Extending the π-system into triethynylethenes (e.g., **70**) and tetraethynylethenes (e.g., **2**, **31b**,**c**) results in concomitant red shifts owing to the larger conjugated systems. A computational study by Lüthi and

Table 1. Longest Wavelength Absorption Maxima (λ_{max}) and Corresponding Energies (E_{max}) for DEEs and TEEs[6,11a,16,22,23,27b,65,66]

compd	solvent	λ_{max} (nm) [ϵ (M^{-1} cm^{-1})]	E_{max} (eV)
(*E*)-**1**	methanol	263 (18100)	4.71
(*Z*)-**1**	methanol	262 (12500)	4.73
2	methanol	330	3.76
24a	*a*	246.8	5.02
31b	ethanol	331 (33900)	3.75
31c	ethanol	349 (35500)	3.55
(*E*)-**66**	tetrahydrofuran	287.5 (40800)	4.31
(*Z*)-**66**	tetrahydrofuran	288.4 (27800)	4.30
(*E*)-**67**	chloroform	296.4 (19700)[b]	4.18
69	chloroform	265 (16500)	4.68
70	hexane	303 (2368), 292 (24914)	4.09

[a] Solvent not reported. [b] Absorption maximum obtained by deconvolution.

co-workers revealed that the difference between linear and cross-conjugation is not only due to the vertical π-conjugation but also to in-plane σ-hyperconjugation (Chart 4).[67]

Chart 4

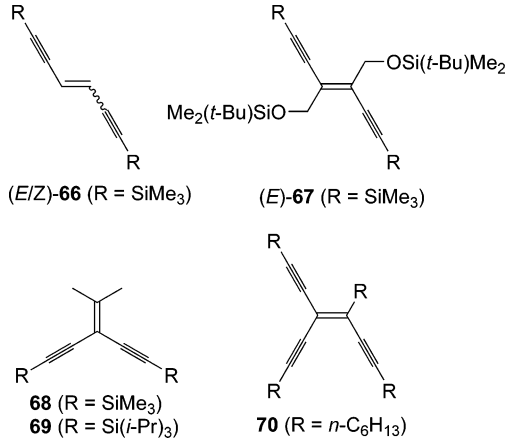

It is known that acetylenic C≡C triple bonds are not reducible electrochemically in organic solvents when they are isolated in molecules, whereas they may undergo reductive electron transfers when entering π-electron interactions with other multiple bonds or conjugated systems.[40e,68,69] Accordingly, TEEs and DEEs can be reduced electrochemically.[40e,56,65,69] The silylated TEE **31c** is reduced at −1.96 V vs Fc^+/Fc in tetrahydrofuran (THF) (one-electron uptake), whereas DEE (*E*)-**67** is reduced at −2.68 V in THF. The more conjugated TEE core is obviously a significantly better electron acceptor than the DEE core.

4.2. X-ray Crystal Structures of DEEs and TEEs

A large selection of X-ray crystal structures of DEEs and TEEs has been reported in the literature.[70] The length of the central C=C double bond in the TEE and DEE cores usually varies between 1.32 and 1.37 Å, whereas the C≡C triple bond lengths vary between 1.17 and 1.22 Å. In Table 2, selected bond lengths and angles for three representative compounds, (*E*)-**71**,[65] **68**,[66] and **31c**,[27b] are collected (Figure 1). The angles at the acetylenic moieties are slightly distorted from the ideal 180° in the solid state likely as a result of crystal packing effects, and the bond lengths and angles listed in Table 2 are average values. The conjugated section is planar in all three structures with only very slight deviations. One notable feature is the small vinylidene angle C2−C3−C5 of 112.9° in the geminal enediyne **68**. Moreover, the triple bonds are more distorted from linearity in this molecule. Overall, the geometrical parameters are in good agreement with those obtained from gas phase ab initio calculations.[40b,71]

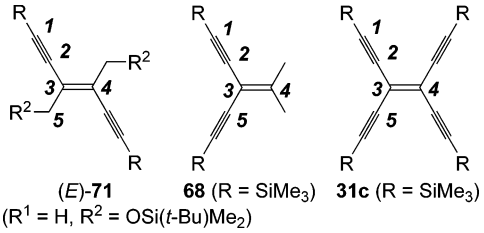

Figure 1. Selected structures investigated by X-ray crystallography. Bond lengths and angles are listed in Table 2.

4.3. Arylated DEEs, Triethynylethenes, and Tetraethynylethenes

As revealed electrochemically, the DEE and TEE cores are electron acceptors, and functionalization by donor units, such as 4-(dimethylamino)phenyl (DMA), results in intramolecular donor−acceptor chromophores with low energy charge transfer (CT) bands (Table 3).[60a,72,73] Accordingly, (*E*)-**72** exhibits an intramolecular CT band at λ_{max} = 397 nm. The CT band is further red-shifted in (*E*)-**73** (λ_{max} = 424 nm) that contains one DMA donor and one 4-nitrophenyl acceptor substituent. For the geminal DEE **74**, where the donor and acceptor groups are situated in a cross-conjugated fashion, an intense band is found at λ_{max} = 325 nm. The absorption extends out beyond 450 nm, possibly owing to "tailing" of a hidden shoulder absorbance (Chart 5).

Aryl-substituted TEEs, such as **77**−**80**,[60a] have broad low energy absorption bands with end absorptions extending beyond 550 nm, characteristic for CT transitions. In the series of donor-substituted TEEs, a significant red shift is observed for (*E*)-**77** (λ_{max} =

Table 2. Bond Lengths and Angles from X-ray Crystallography[27b,65,66]

	bond length (Å)[a]			bond angle (°)[a]		
compd	C1−C2	C2−C3	C3−C4	C1−C2−C3	C2−C3−C4	C2−C3−C5
(*E*)-**71**	1.163	1.426	1.350	176.4	121.3	115.6
68	1.204	1.445	1.348	174.3	124.5	112.9
31c	1.185	1.452	1.324	179.0	121.8	116.5

[a] For atom numbering, see Figure 1. Average values.

Table 3. Longest Wavelength Absorption Maxima (λ_{max}) and Corresponding Energies (E_{max}) for Arylated DEEs and TEEs[a] [60a,72,73]

compd	λ_{max} (nm) [ϵ (M^{-1} cm^{-1})]	E_{max} (eV)	compd	λ_{max} (nm) [ϵ (M^{-1} cm^{-1})]	E_{max} (eV)
(*E*)-**72**	397 (51400)	3.12	(*E*)-**77**	459 (41000)	2.70
(*E*)-**73**	424 (25000)	2.92	(*E*)-**78**	468 (31200)	2.65
74	325 (34000)	3.82	(*Z*)-**78**	471 (17000)	2.63
75	366	3.39	**79**	428 (51100)	2.90
76	366	3.39	**80**	447 (19900)	2.77

[a] Solvent: chloroform.

459 nm) as compared to its geminally oriented counterpart **79** (λ_{max} = 428 nm). The effect of linear conjugation between the two donor groups vs cross-conjugation is also reflected in the redox behavior. Thus, linear conjugation facilitates the oxidation of the anilino groups, since the oxidation occurs at +0.35 V vs Fc^+/Fc (two electrons) for (*E*)-**77** and at +0.42 V (two electrons) for **79**. In contrast, the reduction occurs at very similar potential for the two compounds (ca. −2.0 V). Consequently, the smaller highest occupied molecular orbital (HOMO)−lowest unoccupied molecular orbital (LUMO) gap observed for (*E*)-**77** is a result of an increase in the HOMO energy via efficient linear conjugation between the two aryl groups. For donor−acceptor functionalized TEE derivatives, a red shift is also observed when proceeding from linearly conjugated aryl groups in (*E*)-**78** (λ_{max} = 468 nm) and (*Z*)-**78** (λ_{max} = 471 nm) to cross-conjugated aryl groups in **80** (λ_{max} = 447 nm).

Protonation of the dimethylamino groups by treatment with concentrated aqueous HCl leads to a complete loss of the CT transitions. The spectra exhibited longest wavelength maxima around 380 nm, typical of Ph- or *p*-$C_6H_4NO_2$-substituted TEEs.[70g] The quenching of the CT absorptions by protonation is reversible. Thus, treatment of the protonated forms with aqueous NaOH regenerated the neutral species, and the UV/vis spectra became virtually identical to those measured before the acid treatment.

The UV/vis spectra of the three isomeric products **31a**, **32a**, and **33a** reported by Hori et al. could provide evidence for cross-conjugation being effective,[21] since these compounds exhibit very similar longest wavelength absorptions (at ca. λ_{max} = 410 nm) despite their different linear conjugation lengths. This observation signals that all of the π-electrons in these planar compounds are delocalized to almost the same extent. The planarity of tetrakis(phenylethynyl)ethene **31a** was confirmed by X-ray crystallography by Hopf and co-workers.[58] The extensive number of X-ray crystal structures of TEE and DEE derivatives[70] have revealed fully or nearly planar π-conjugated carbon cores, which, in most cases, also includes terminal aryl rings. In some solid state structures, terminal aryl rings are not in plane with the central core, presumably due to crystal packing effects. In these cases, they adopt an orthogonal orientation, thereby maintaining conjugation with the second set of π-orbitals in the adjacent C≡C bond. The molecular structures of donor−acceptor substituted TEEs (*E*)- and (*Z*)-**78** showed little indication of an intramolecular ground state CT, and bond lengths and angles of their TEE cores were in the range of those seen in other derivatives. The bond length alternation in the DMA rings is a good indication for the CT from the DMA donor to the TEE acceptor moiety, which can be expressed by the quinoid character (δr) of the ring defined by[74]

$$\delta r = [(a - b) + (c - b)]/2 \approx [(a' - b') + (c' - b')]/2$$

where *a*, *b*, and *c* are defined according to Figure 2. In benzene, the δr value equals 0, whereas values between 0.08 and 0.10 are found in fully quinoid rings. The δr values for DMA rings in donor−acceptor substituted TEEs, calculated from several X-ray structures, generally do not exceed 0.025.

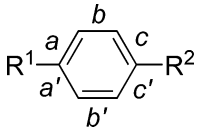

Figure 2. Definition of bond lengths for calculation of quinoid character (δr).

Chart 5

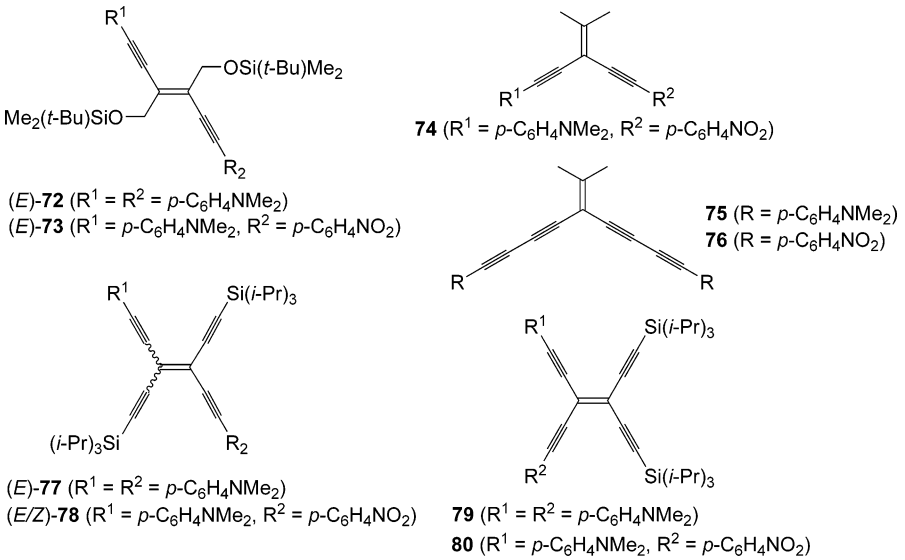

Arylated TEEs exhibit exceptionally high third-order optical nonlinearities;[75] this property is rooted in the coplanarity of the TEE core and the aryl substituents, which allows full two-dimensional conjugation over the entire chromophore.[76]

4.4. Bis-DEEs and Bis-TEEs

Linking two units of (*Z*)-**1** together results in a significant red shift of the longest wavelength absorption. Thus, the longest wavelength absorption of **63** is at $\lambda_{max} = 347$ nm (Table 4),[77] while it is at $\lambda_{max} = 262$ nm for (*Z*)-**1**. Table 4 lists the absorption maxima for a variety of simple bis-DEEs.[11h,77−81] Comparing linearly conjugated (*Z*)- and (*E*)-bis-DEEs **82** and **83** with the same substitution pattern, we notice that the *E*-configuration (**83**) leads to a slightly lower HOMO−LUMO gap. Cross-conjugated dimers **84**−**86** exhibit higher HOMO−LUMO gap energies. In contrast, the HOMO−LUMO energy is very small in TEE dimer **87** (Chart 6).

Table 4. Longest Wavelength Absorption Maxima (λ_{max}) and Corresponding Energies (E_{max}) of DEE and TEE Dimers[11h,77−81]

compd	solvent	λ_{max} (nm) [ϵ (M^{-1} cm^{-1})]	E_{max} (eV)
63	diethyl ether	347 (21200)[a]	3.57
81	hexane	366 (29700)	3.39
82	chloroform	364 (15500)	3.41
83	chloroform	369 (27600)	3.36
84	chloroform	337 (14400)	3.68
85	chloroform	340 (11500)	3.65
86	chloroform	329 (22300)	3.77
87	hexane	432 (35500)	2.87
88	chloroform	547 (sh, 32300)	2.27

[a] Mimimal value due to the instability of the compound.

Chart 6

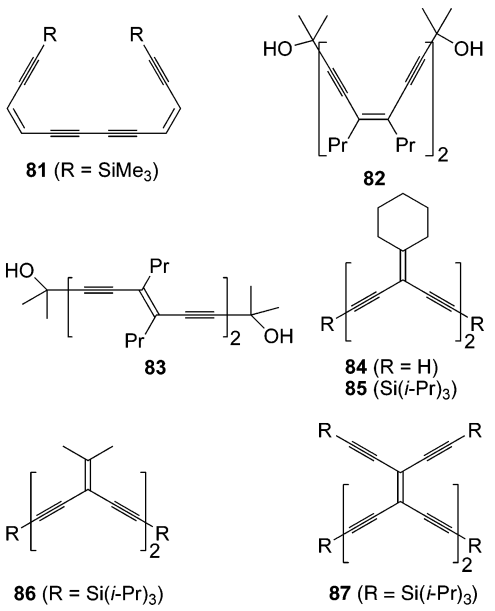

Electrochemical studies reveal that linking two TEE units together to form **87** containing a C_{20} core enhances the acceptor strength considerably.[80] Thus, according to cyclic voltammetry, compound **87** experiences reversible reductions at −1.52 and −1.89 V and an irreversible reduction at −2.90 V vs Fc^+/Fc in THF. The acceptor strength is also deduced from UV/vis spectroscopic studies of donor-substituted derivatives. Thus, DME-functionalized TEE dimer **88** experiences a CT band at $\lambda_{max} = 547$ nm (Chart 7).[81]

Chart 7

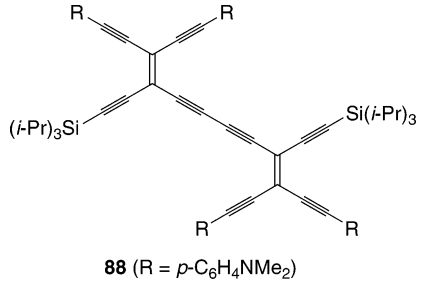

4.5. Cyanoethynylethenes (CEEs)

An ultimate tuning of the acceptor strength, while maintaining the opportunity for acetylenic scaffolding, can be achieved by functionalization with cyano groups.[82] Thus, the CEEs **89**−**96**[82e] show first reduction potentials in the range between that of TEE derivative **31c** (−1.96 V vs Fc^+/Fc in THF) and tetracyanoethene (TCNE, −0.32 V in CH_2Cl_2).[83] In substituted TEEs, the 4-nitrophenyl group essentially acts as an independent redox center and an increase in the number of these substituents does not increase the acceptor strength of the chromophore.[40e] In sharp contrast, the cyano group in CEEs is an integral part of the acetylene-based chromophores and the first reduction potential shifts strongly anodically with an increasing number of cyano groups. The increase in electron acceptor strength upon substituting one RC≡C− by one N≡C− group can be quantified to 380 mV and upon replacing one RC≡C−C−C≡CR by one NC−C−CN fragment to 830 mV (Chart 8).[84]

A clear increase in acceptor strength with extension of π-electron conjugation is observed when proceeding from monomer **91** to dimer **96**, as was likewise found when proceeding from TEE monomer **31c** to TEE dimer **87**. Thus, the extended CEE **96** is an exceptionally good electron acceptor with a first reduction occurring at −0.57 V vs Fc^+/Fc in CH_2Cl_2, approaching the strength of TCNE.

Recently, donor-substituted CEEs **97**−**103** were prepared and characterized.[82f] These molecules display exceptionally strong intramolecular CT interactions. The oxidation of the anilino group in **97** occurs at a very anodically shifted potential (+0.79 V) as compared to an anilino group attached to a TEE core (+0.3−0.5 V), and it implies that the anilino moiety and the CEE core do not act as independent redox entities but rather undergo strong electronic communication (Chart 9).

X-ray crystallographic analysis of **97** and **100** reveals planar CEE cores.[82f] In the case of **96**, the phenyl rings are twisted out of the main plane by ca. 14°. CEE **100** exhibits a quinoid character with a δr of 0.033, and **97** has a value of 0.037. These values clearly demonstrate a highly enhanced intramolecular ground state CT in the CEEs as compared to the TEEs.[82g]

Chart 8

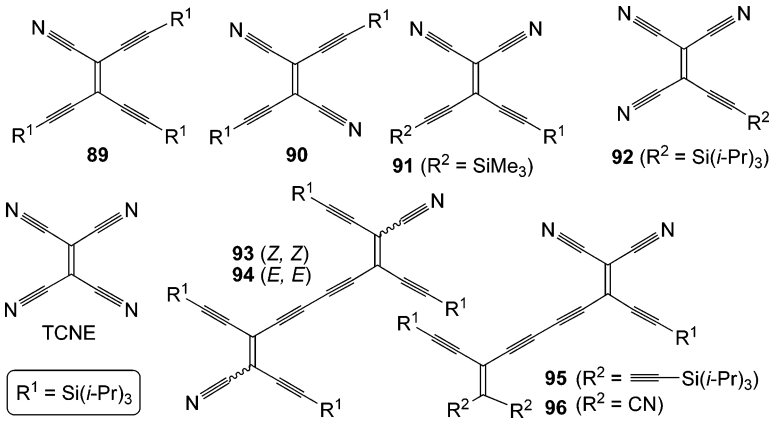

Chart 9

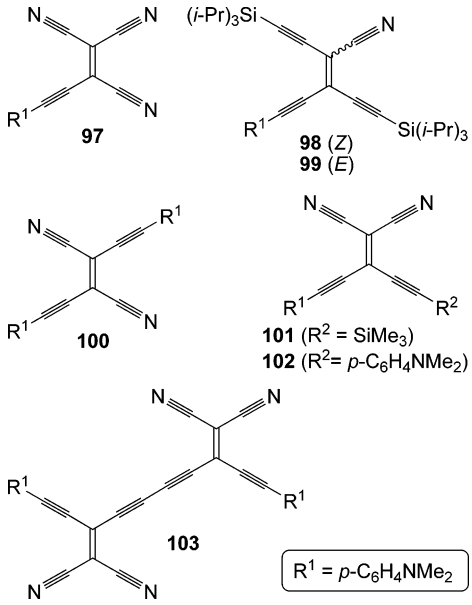

Chart 10

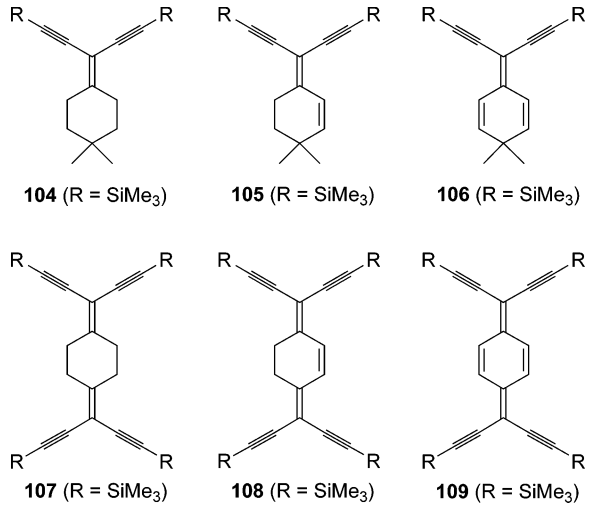

5. Derivatives of Tetraethynyl-*p*-quinodimethane

Hopf and co-workers[85] prepared a selection of conjugated molecules derived from *gem*-**1** via cross-coupling between terminal acetylenes and vinylic dibromides. The molecules **104**−**108** are examples of this class. The 7,7,8,8-tetraethynyl-*p*-quinodimethane **109** was prepared by Neidlein and Winter.[86] From UV/vis absorption spectra, it transpires that cross-conjugation contributes to the total π-electron delocalization in these molecules (Table 5). Thus, significant red shifts are observed when proceeding along the series **104**, **105**, **106**, or along the series **107**, **108**, **109**. It is also interesting to compare **109** with TEE **31c** containing the same outer trimethylsilyl substituents: Extending the ethene spacer results in a significant red shift from $\lambda_{max} = 349$ (**31c**) to 565 (**109**) nm. Interestingly, compound **106** exhibits a longest wavelength absorption maximum similar to **31c**, the major difference being the substitution of two triple bonds for two double bonds about the central ethene unit. Nevertheless, the tetravinylethylene **110** shows a λ_{max} at 284 nm,[87] which is, accordingly, significantly blue shifted relative to the parent TEE **2** ($\lambda_{max} = 330$ nm), presumably as a result of structural nonplanarity (Charts 10 and 11).

Table 5. Longest Wavelength Absorption Maxima (λ_{max}) and Corresponding Energies (E_{max}) of Extended *gem*-DEEs[85−87]

compd	solvent	λ_{max} (nm) [ϵ (M^{-1} cm^{-1})]	E_{max} (eV)
104	pentane	266 (19100)	4.66
105	pentane	308 (24500)	4.03
106	pentane	354 (sh, 23400)	3.50
107	pentane	292 (sh, 24500)	4.25
108	pentane	354 (sh, 23400)	3.50
109	hexane	565 (6920)	2.19
110	ethanol	284 (23300)	4.37

Chart 11

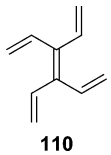

6. Conjugated Oligomers

6.1. Linearly Conjugated Oligomers

PA (**111**) is the simplest conjugated polymer[88] with an all-carbon backbone not composed of aromatic rings and has been extensively exploited for its electrical conductivity upon doping.[89] Poly(diacetylene)s (PDAs, **112**) and poly(triacetylene)s (PTAs,

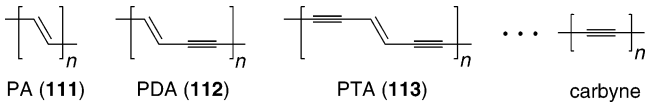

Figure 3. Progression from polyacetylene (PA) to carbyne.

Chart 12

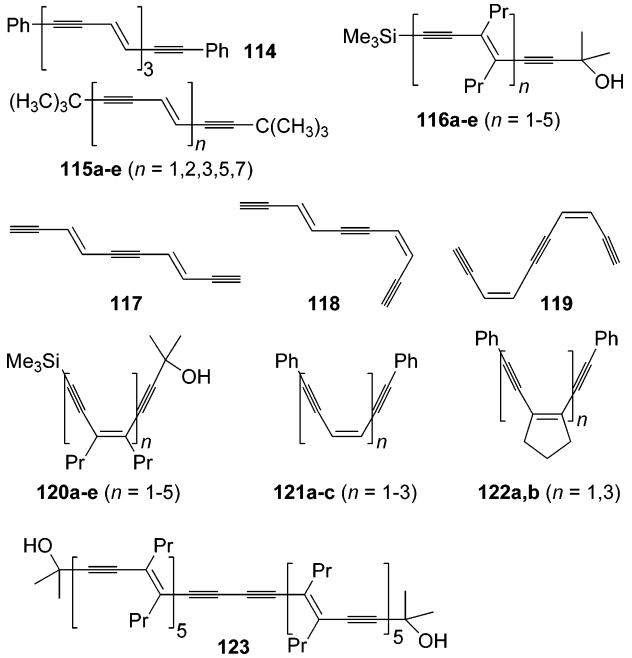

113), which both contain DEEs in the π-chain, are the next representatives in a progression, which ultimately leads to carbyne (Figure 3). The direct analytical characterization and physical study of extended π-chain polymers with high molecular weight are often hindered by low solubility. Structural defects are also common obstacles preventing the acquisition of sound physical data. Soluble, monodisperse oligomers serve as finite model systems and offer the possibility to attain specific information by extrapolation of the electronic, photonic, thermal, and morphological properties of the corresponding polydisperse high molecular weight analogues.[90] Moreover, the systematic study of oligomers with precisely defined length, constitution, and conformation allows direct correlation of physical properties with chemical structures and enables the generation of useful and predictive structure−property relationships. The study of well-defined monodisperse oligomers has also advanced into a strong field of its own right, because of the promising electronic and optical properties of these compounds. Thus, these molecular wires could serve as potential components in future molecular scale electronic devices.[91]

Oligomerization of suitably functionalized DEEs has provided a large selection of linearly conjugated PDA[11g,h,92−95] and PTA[11h,i,65,80,96] oligomers. The compounds **114**,[93] **115a**−**e**,[92b] **116a**−**e**,[11g,h] **117**−**119**,[94] **120a**−**e**,[11g,h] **121a**−**c**,[95] and **122a**,**b**[95] represent examples of PDA oligomers that have been prepared and characterized. Compound **123**[11g,h] is a PDA−PTA hybrid oligomer consisting of two pentameric PDA backbones linked together by a buta-1,3-diynediyl bridge. Compounds **124a**−**h**,[96f,h] **125a**−**e**,[11h] and **126a**−**e**[11h] are PTA oligomers based on either *E*- or *Z*-DEEs, whereas PTAs **127a**−**e**,[80] **128a**−**e**,[80,96a] and **129**[96b] are based on TEE repeat units (TEE-PTAs). With an estimated length of 17.8 nm, the 24-mer **124h** is the longest known molecular rod featuring a fully conjugated, nonaromatic all-carbon backbone (Charts 12 and 13).[96h]

The energy (E_{max}) corresponding to the longest wavelength absorption maximum (λ_{max}) for PDA and PTA oligomers is plotted as a function of the number (n) of monomeric repeat units in Figures 4 and 5, respectively. From such plots, the effective conjugation length (ECL) can be evaluated; that is, the number of monomeric units at which saturation occurs and E_{max} of an infinite polymer can be predicted. Although saturation does not occur abruptly at a specific number of monomer units, we shall evaluate ECLs in this simplified manner. A more concise picture of the length dependence of the optical absorption of conjugated systems has been given by Rissler.[97] Moreover, the different properties of a conjugated system (e.g., absorption maximum, fluorescence maximum, oxidation potential, reduction potential, and nonlinear optical properties) do not necessarily saturate to the same extent with increasing chain length. The ($1/n$, E_{max}) plots of (*E*)-PTAs **124b**−**h** and **125b**−**e**, (*Z*)-PTAs **126b**−**e**, and TEE-PTAs **127b**−**e** show approximately linear regimes for "medium-sized" molecules that flatten out at small

Chart 13

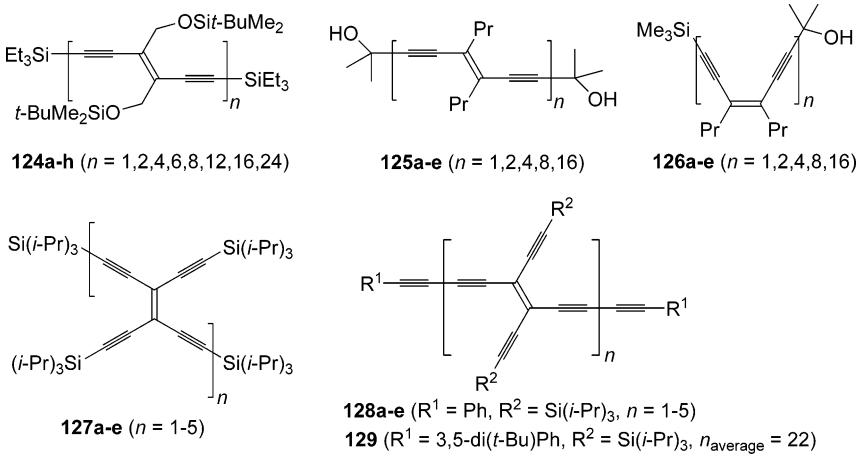

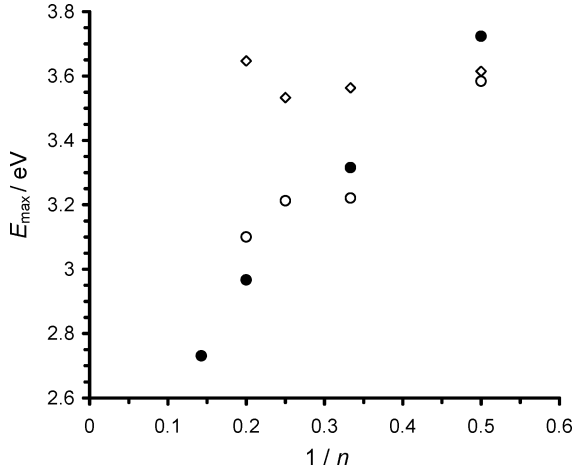

Figure 4. Plots of E_{max} vs $1/n$ to extrapolate the optical band gaps for infinite PDA polymers: PDA oligomers **115b**−**e** (●), **116b**−**e** (○), and **120b**−**e** (◇). E_{max} corresponds to the longest wavelength absorption maximum λ_{max}. n = number of monomeric repeat units in the oligomers.

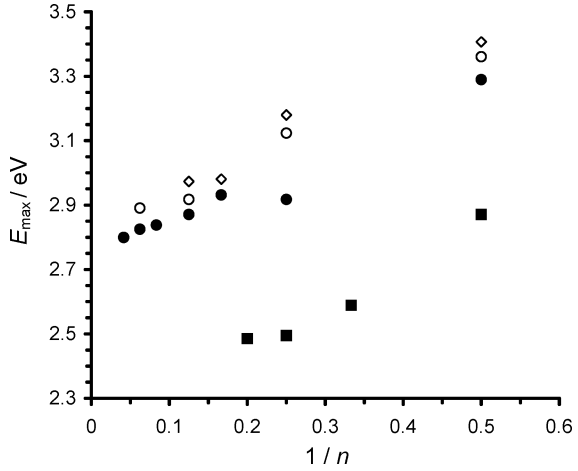

Figure 5. Plots of E_{max} vs $1/n$ to extrapolate the optical band gaps for infinite PTA polymers: PTA oligomers **124b**−**h** (●), **125b**−**e** (○), **126b**−**e** (◇), and **127b**−**e** (■).

Table 6. Comparison of Longest Wavelength Absorption Energies E_{max} (Corresponding to λ_{max}) Obtained from Oligomer Extrapolation or Directly from Polymer[a]

	oligomers	ECL	E_{max} (eV) from oligomer extrapolation	E_{max} (eV) for polymer
(*E*)-PA			1.8[c]	1.8 (1.4)[b]
(*E*)-PDA	**115b**−**e**, **116b**−**e**	6,[c] 10[e]	2.3[d,e]	2.3/1.9[g]
(*Z*)-PDA	**120b**−**e**	2	3.6	
(*E*)-PTA	**124b**−**h**, **125b**−**e**	10	2.8 (2.5)	2.8[f]
(*Z*)-PTA	**126b**−**e**	8	3.0	
TEE-PTA	**127b**−**e**	4	2.5	

[a] ECL (i.e., number of repeat units) obtained from oligomer extrapolation. Values in brackets are absorption edge energies. [b] Ref 88a. [c] Ref 92a. [d] Ref 92b. [e] Ref 92c. [f] Ref 96e. [g] An absorption at λ = 650 nm (1.9 eV) is ascribed to unusual solid state effects; ref 92b,c.

$1/n$ values, i.e., for longer oligomers, which allow determination of the ECL as defined above. Values are collected in Table 6 and compared with those determined for the polymers.[88a,92] The two values for the ECL of (*E*)-PDA were obtained by Wenz et al.[92a] and Giesa et al.,[92c] respectively, from different plots as the one used here and via comparison to the polymer absorption. The data in Table 6 reveal that the (*Z*)-oligomers have higher optical gaps than the (*E*)-oligomers and exhibit smaller ECLs. In particular, the difference is very significant in the PDA series, presumably due to nonplanarity of the (*Z*)-oligomers. We also notice that substituting double bonds for triple bonds along the progression of PA, PDA, and PTA results in a concomitant increase in the transition energy. Moreover, the TEE-based PTAs **127a**−**e** exhibit extremely small optical gaps and meet saturation already at four repeat units.

X-ray crystallographic analysis of the PTA 4-mer **124c** shows that the conjugated system is perfectly planar, with the squared sum of the deviations of the backbone C-atoms from the best plane amounting to 0.077 Å^2.[96h] Nevertheless, UV/vis studies on PTA oligomers, dendritically encapsulated with bulky wedges, revealed that the electronic properties were unchanged upon distorting the backbone out of planarity as a result of steric compression of the dendritic wedges.[96c,g]

End functionalization with aryl groups in the PTA series results in a red shift of the longest wavelength absorption maximum. Thus, PTAs **128a**−**c** exhibit longest wavelength absorption energies of 2.59, 2.59, and 2.45 eV, respectively.[80,96a] This lower energy absorption reflects the extension of the π-chromophore upon introduction of the peripheral aryl groups. For comparison, the absorption energies of the aryl end-capped poly(pentaacetylene)s **130a**−**c** are 2.71, 2.44, and 2.39 eV, respectively (Chart 14).[96g]

Chart 14

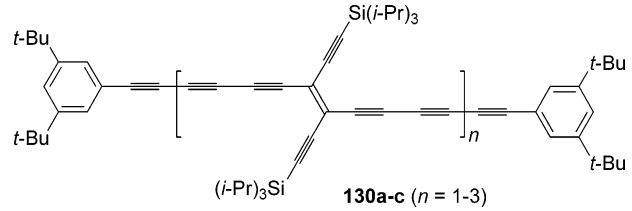

130a-c (n = 1-3)

Cyclic voltammetry reveals that proceeding along the PTA series **128a**−**e** causes a continuous drop of the first reduction potential to less negative potentials. Thus, the 5 nm long pentamer **128e** is a very strong electron acceptor with the first reduction occurring at −1.07 V vs Fc^+/Fc in THF. For polymer **129**, containing an average of 22 TEE units, the first reduction occurs already at −0.70 V.[96b] Each oligomer **128a**−**e** exhibits a number of reversible or quasi-reversible one-electron reduction steps that are equal to the number of TEE moieties in the backbone. Figure 6 shows the changes in the reduction potentials along the series.

6.2. Cross-Conjugated Oligomers

Dendralenes are polyene hydrocarbons in which all C=C bonds are aligned in a cross-conjugated arrangement.[98] Upon formal insertion of one or more acetylene units between the C=C bonds, series of expanded dendralenes are obtained. Dendralenes and expanded dendralenes are also conveniently termed

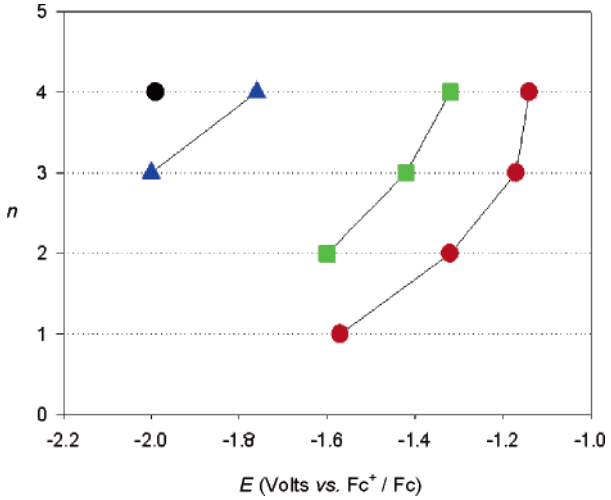

Figure 6. Changes in the reduction potentials (vs Fc^+/Fc) measured for the monomer and oligomers of PTAs **128a**–**d** in THF + 0.1 M Bu_4NPF_6: first (red circles), second (green squares), third (blue triangles), and fourth (black circle) reduction step. Reprinted with permission from ref 69. Copyright 2004 Wiley-VCH.

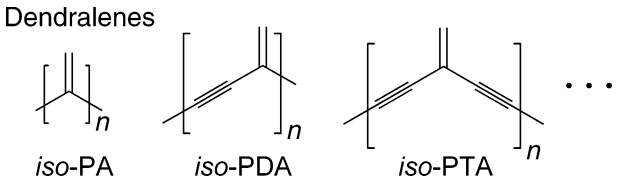

Figure 7. Definition of dendralenes and expanded dendralenes, *iso*-PAs, *iso*-PDAs, *iso*-PTAs, etc.

iso-PAs, *iso*-PDAs, etc. (Figure 7).[99] A large selection of expanded dendralenes containing the *gem*-DEE or *gem*-TEE units has been prepared, such as **131a**–**i**,[19a,66] **132a**–**d**,[78] **133a**–**c**,[79] **134**,[79] and **135a**–**c**,[80] as well as hybrid systems, such as **136a**–**d** (Chart 15).[79,100]

Optical gaps (E_{max}) for the series **131b**–**i**, **132b**–**d**, and **135a**–**c** are plotted as a function of the number of repeat units in Figure 8.[101] The extrapolated values for infinite polymers are collected in Table 7.[102] It transpires that the optical gaps are significantly larger in the cross-conjugated oligomers as compared to their linearly conjugated counterparts. Moreover, we observe again that oligomers based on TEE repeat units provide the smallest optical gaps.

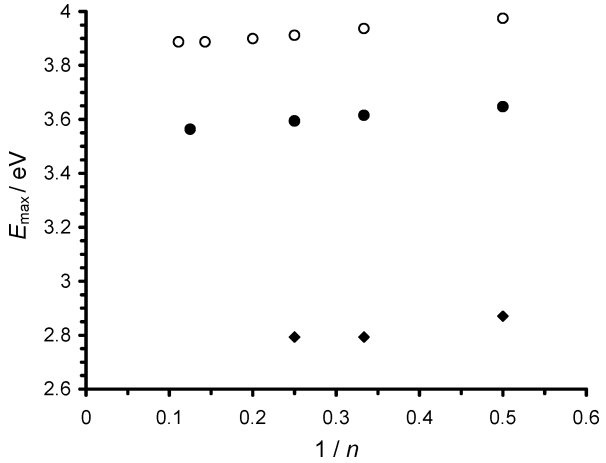

Figure 8. Plots of E_{max} vs $1/n$ to extrapolate the optical band gaps for infinite expanded dendralene polymers: expanded dendralenes **131b**–**i** (○), **132b**–**d** (●), and **135a**–**c** (◆).

Table 7. Longest Wavelength Absorption Energies E_{max} (Corresponding to λ_{max}) and Effective Conjugation Lengths ECL (i.e., Number of Repeat Units) Obtained from Oligomer Extrapolation[a]

	oligomers	ECL	E_{max} (eV) from oligomer extrapolation
iso-PA	dendralenes	2[b]	5.6[b]
iso-PDA	**131b**–**i**	9	3.9[c] (3.8)
iso-PTA	**132b**–**d**	10	3.5 (3.3)
iso-TEE-PTA	**135a**–**c**	3	2.8

[a] Values in brackets are absorption edge energies. [b] Ref 98. [c] Corresponding to the wavelength at $\epsilon_{max}/2$ at the lower energy tail of the absorption band; see ref 101.

The lower energy region of the absorption spectra of tetrayne-based oligoenynes **136a**–**d** is dominated by the absorption pattern of the tetrayne moiety.[79,100] Each tetrayne exhibits three identical absorptions at λ_{max} = 405, 374, and 348 nm. These absorptions are found at virtually identical energies for other tetraynes such as 1,8-bis(4-*tert*-butylphenyl)octatetrayne. No obvious energy shift (less than 1 nm) is observed in the tetrayne absorptions as a result of increasing the cross-conjugated chain length from **136a** to **136d**. However, the higher energy absorptions resulting from the *iso*-PTA segments of the molecules (ca. 330 nm) show a slight bathochromic shift in the longer oligomers. Thus, with chain

Chart 15

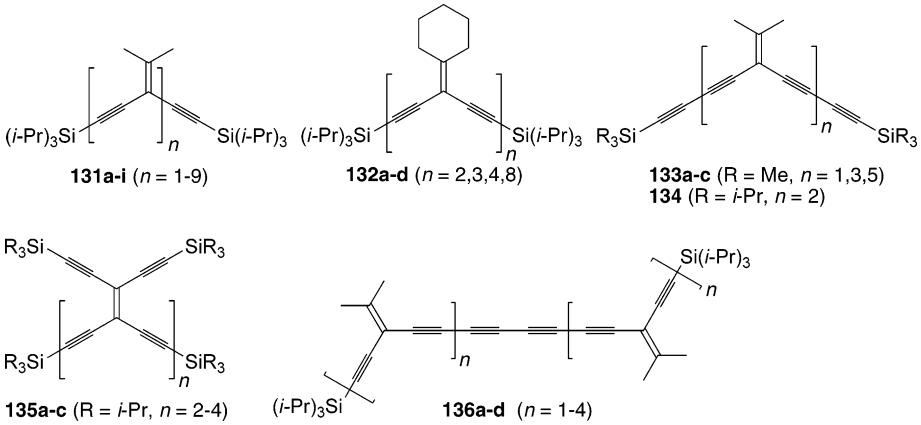

Chart 16

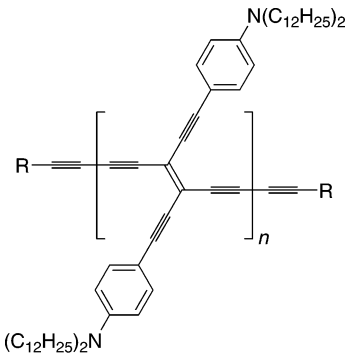

137 (R = 3,5-di(*t*-Bu)Ph, $n_{average}$ = 22)

elongation, a merging ultimately occurs of the *iso*-PTA absorption with that of the tetrayne moiety at 348 nm, affording a single, nondistinctive shoulder for **136d**.

6.3. Donor–Acceptor Functionalized DEE-PTAs

6.3.1. Influence of Lateral Functionalization

The effect of lateral aryl donor functionalization can be ascertained by comparing the two PTAs **129** and **137**,[96b] the first containing lateral silyl groups and the second containing lateral anilino groups. The degrees of polymerization (average number of monomeric repeat units $n_{average}$) were determined by ^{1}H NMR signal integration. Comparison of their physical properties reveals a significant enhancement upon lateral donor functionalization, e.g., of the NLO response. Thus, the solution state longest wavelength absorption energy of **137** (E_{max} = 1.6 eV) is substantially reduced relative to that of **129** (E_{max} = 2.0 eV). The PTA **137** only gave one irreversible reduction at −1.28 V (vs Fc/Fc$^+$ in CH_2Cl_2), being anodically shifted by +330 mV relative to the first reduction of TEE dimer **88**. Thus, the longer linear conjugation length in **137** facilitates the first reduction relative to **88**. Moreover, as generally observed for anilino-substituted TEE scaffolds, **137** undergoes reversible oxidation centered on the anilino groups ($E°$ = +0.45 V, vs Fc/Fc$^+$ in CH_2Cl_2) (Chart 16).

6.3.2. Influence of Spacer Units

The modulation of the electronic properties of PTA oligomers by π-electron-deficient and -rich aromatic and heteroaromatic spacer units has been tested in a large variety of compounds.[103,104] The extended DEE dimers **138a**–**n** and **139a**,**b** represent examples of such compounds.[103c,e] Insertion of spacers had a profound influence on their molecular properties, such as fluorescence behavior. Thus, whereas the luminescence quantum yields of compounds **139a**,**b** and hybrid trimer **138j** were below 5% in chloroform (λ_{exc} = 356 nm), hybrid derivatives **138a**, **138e**, **138g**, and **138i** featured quantum yields between 20 and 50%. The yields were even increased above 50% in hybrid trimers **138b**–**d**, **138f**, and **138h**. Furthermore, the benzothiadiazole-containing compound **138k** shows by far the highest yield of 80%. An extremely

Chart 17

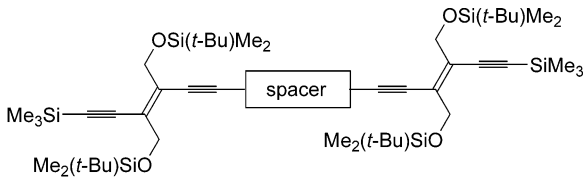

138a-n, **139a,b**

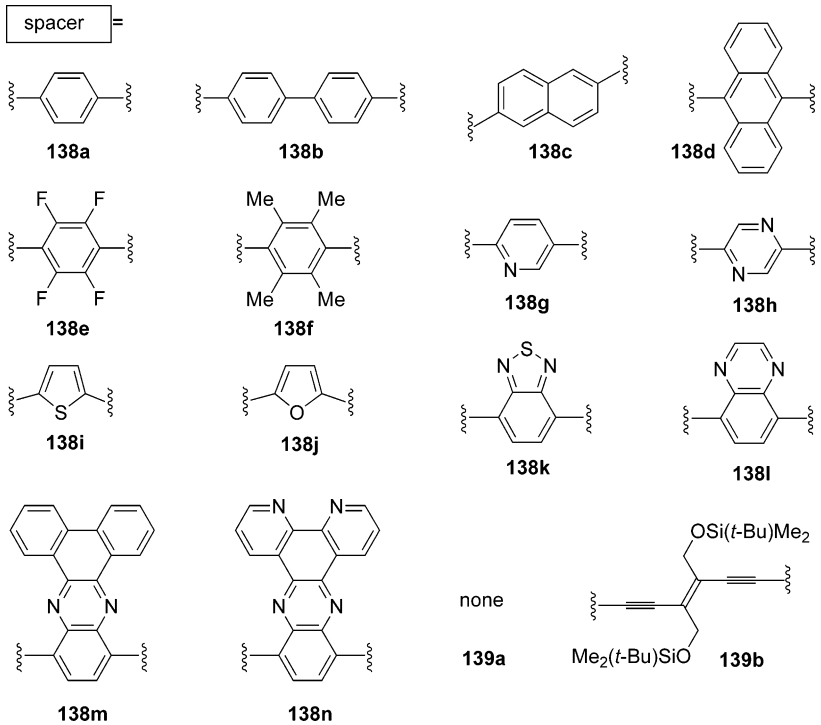

Chart 18

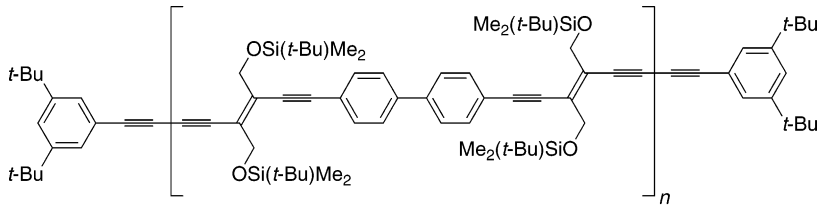

140 ($n_{average}$ = 19)

enhanced emission is also observed for the quinoxaline derivatives **138l**−**138n** (yields between 65 and 75%). Complexation of **138n** with transition metal ions leads to a red shift of the emission band and a decrease in the fluorescence quantum yield. Thus, the [Ni(**138n**)(ClO_4)$_2$] complex only shows a yield of 3% (Chart 17).

Whereas DEE trimer **139b** experiences a large bathochromic shift of the longest wavelength absorption maximum relative to that of DEE dimer **139a** [λ_{max} = 407 nm, shoulder (**139b**), λ_{max} = 376 nm (**139a**)], hybrid trimers **138a**−**c** display about the same longest wavelength absorption maxima, as well as end absorptions, as **139a**. Thus, benzenoid spacers are less effective in transmitting π-electron delocalization along the oligomeric backbone. In contrast, introduction of the anthracene spacer in **138d** brings about a red shift of all bands in the UV/vis spectrum, which in the longer wavelength region resembles the characteristic spectrum of anthracene itself. This enhanced conjugation reflects the small loss in aromaticity in going from the aromatic to the quinoid resonance structure of this spacer. The same effect has been observed for other systems. Thus, Müllen and co-workers[105] have shown that the incorporation of anthracene spacers in conjugated polymers reduces the band gap. Moreover, Anderson and co-workers[106] found enhanced conjugation in anthracene-linked porphyrins. Insertion of electron-rich heterocyclic spacers as in thiophene derivative **138i** and furane derivative **138j** results in very efficient π-electron delocalization, changing the longest wavelength absorption maximum to 404 (shoulder) and 398 (shoulder) nm, respectively. While a pyridine spacer (in **138g**) does not produce a bathochromic shift, the pyrazine-spaced compound **138h** experiences a longest wavelength absorption at λ_{max} = 392 nm (shoulder). Indeed, the benzenoid aromaticity is more pronounced in pyridine than in pyrazine. Pyridine derivative **138g** represents an interesting example of a molecular system, in which both the electronic absorption and the emission characteristics can be reversibly switched as a function of pH. Thus, protonation results in a large bathochromic shift of the most intense electronic absorption band from λ_{max} = 337 to 380 nm and a decrease in the fluorescence quantum yield from 40 to 7% (λ_{exc} = 356 nm).[103c]

The first reduction of the quinoxaline compounds **138l** and **138n** is substantially facilitated relative to the free spacer units, by 400 and 240 mV, respectively.[103e] These large anodic shifts likely originate from inductive effects exerted by the two DEE units on the large central spacer chromophore rather than from extended π-electron conjugation. This same effect is observed for porphyrin-extended DEE dimers (vide infra).

A long-chain oligomer (**140**) was prepared based on the biphenyl spacer.[103d] This PTA retained the strong emission behavior of **138b**, displaying a fluorescence quantum yield of 44% in chloroform; such compounds could have potential in light-emitting diodes. It also deserves mention that besides enhancing fluorescence properties, the DEE modules enhance the oligomers' solubility (Chart 18).

Pt−TEE molecular scaffolding has yielded PTA oligomers with Pt(PEt_3)$_2$ as spacer units.[107] Both linear and nonlinear optical properties of the oligomers **141a**−**f**[107c] revealed an almost complete lack of π-electron conjugation along the backbones; that is, the Pt atoms act as insulating centers in these linear systems. Thus, all oligomers display very similar UV/vis spectra. The spectra reveal a strong metal-to-

Chart 19

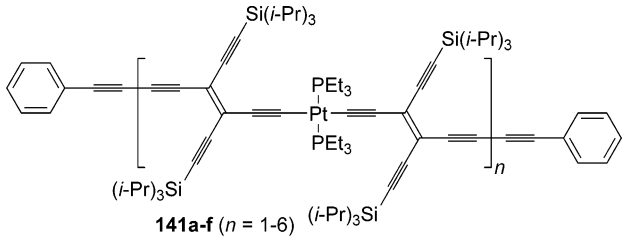

141a-f (n = 1-6)
142 ($n_{average}$ = 31)

Chart 20

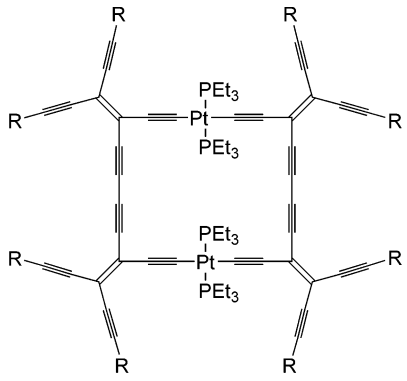

143 (R = 3,5-di(t-Bu)Ph)

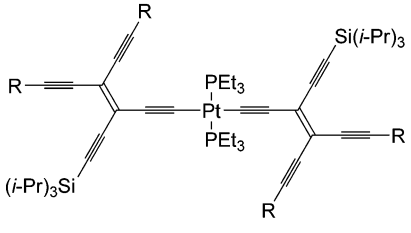

144 (R = 3,5-di(t-Bu)Ph)

ligand CT band dominating the longer wavelength spectral region. Both the maximum of this band and the spectral end absorption shift only slightly to longer wavelengths up to the tetramer, after which saturation of the electronic properties occurs. Thus, λ_{MLCT} moves from 436 (in monomeric **141a**) to 442 (in pentameric **141e**) nm and remains exactly at this wavelength in hexameric **141f**. In agreement with inefficient π-electron conjugation along the linear backbone, the UV/vis spectrum of polymer **142** in CH_2Cl_2 closely resembles the monodisperse oligomers, with λ_{MLCT} appearing at 446 nm. This insulating behavior of the $Pt(PEt_3)_2$ spacer units contrasts with their ability to convey to some extent π-electron delocalization in the macrocyclic complex **143**.[107a,b] The end absorption band of **143** is bathochromically shifted relative to the dimer **144** and extends well beyond 500 nm. Thus, electronic communication may exist along the rectangular perimeter of **143**.[108] The bathochromic shift may on the other hand simply be a result of the existence of butadiyne links in **143** and the conformational constraints of a cyclic system (Charts 19 and 20).

6.3.3. Donor–Donor and Acceptor–Acceptor End-Functionalization

The PTA mono-, di-, tri-, tetra-, penta-, and hexamers **145a**−**f** and **146a**−**f** provide useful information regarding the influence of donor−donor (D−D) and acceptor−acceptor (A−A) substitution in the end groups of PTAs based on the (*E*)-DEE repeat unit.[96d] Compounds **145g** and **146g** (∼18 DEE units) were studied as reference points for the infinitely long polymers. The ECL was estimated from the longest wavelength absorption maxima of the compounds in each of these two series. The electronic properties of the end caps were found to have a strong influence on the ECL. Thus, the ECL of the A−A PTA oligomer **146g** was determined to be $n = 10$, being of the same length as that found for silyl end-capped PTA oligomers. Yet, the D−D PTA oligomer **145g** exhibits a much shorter ECL of only $n = 4$. This decrease in ECL is probably explained by the formation of strong CT bands dominating the absorption properties. Raman scattering measurements suggested an even smaller value of $n = 3$ for this PTA (Chart 21).

Chart 21

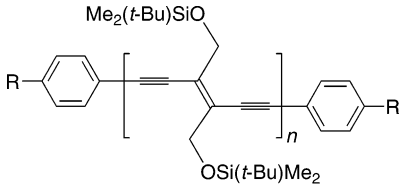

145a-g (R = NMe_2, n = 1-6, ∼18)
146a-g (R = NO_2, n = 1-6, ∼18)

7. Porphyrin Derivatives

The strong electron-withdrawing effect of the DEE unit (vide supra) was confirmed by its ability to alter the electrochemistry of porphyrins, such as **147**, in porphyrin arrays.[103a] Compounds **148** and **149a**,**b** showed two one-electron oxidation and two one-electron reduction waves, all of which were porphyrin-based as evidenced by comparison to the porphyrin derivative **147**. Whereas all three compounds were reversibly oxidized at similar potentials, reductions became significantly facilitated upon increasing DEE substitution. Thus, attachment of two DEE moieties to the porphyrin core in **149a** shifts the first one-electron reduction anodically by 350 mV when compared with **147** lacking these substituents (Chart 22).

Chart 22

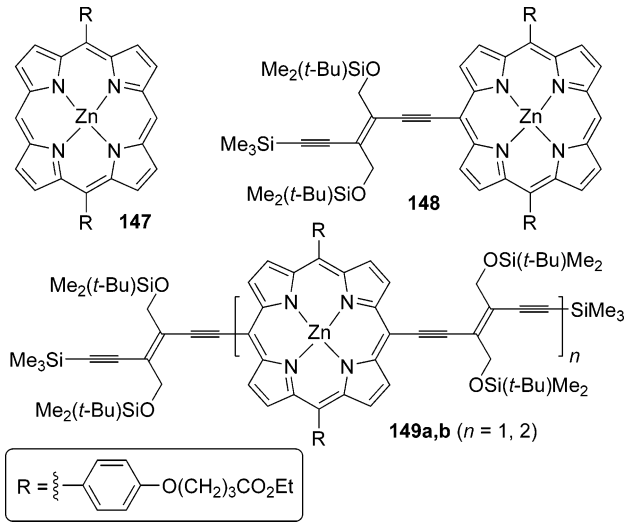

Shultz et al.[18b,109] synthesized the cross-conjugated bis-porphyrins **150** and **151** and studied their properties in comparison to other coupled porphyrins, such as the *m*- and *p*-phenylene-bridged **152** and **153**. Electrochemistry shows that the first oxidation of each porphyrin in **152** and **153** occurs at a nearly identical potential; that is, a single two-electron wave is observed, which indicates that interaction between the radical cations is negligible. One might have expected that the close proximity of the two porphyrins in the *m*-phenylene-bridged compound **152** would have resulted in a redox splitting simply due to electrostatic repulsion between the two radical cations. In contrast, the oxidation of the porphyrin rings in **150** and **151** occurs at different potentials. This splitting of the redox potentials is explained by a communication between the two porphyrins mediated by the *gem*-DEE unit and hence beyond simple electrostatic repulsion (Chart 23).

Chart 23

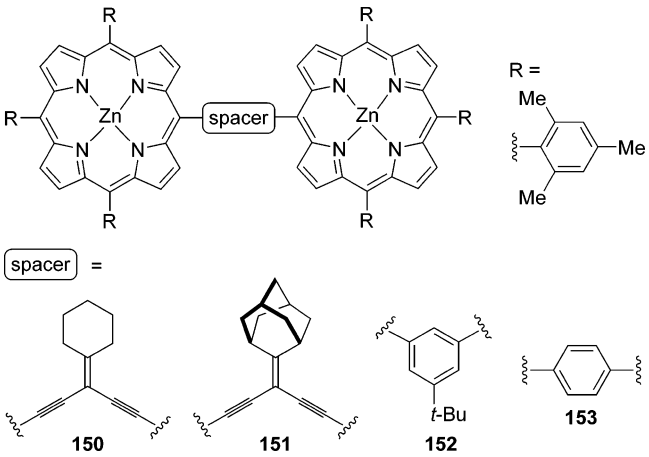

Scheme 16. Reversible Oxidations of TTF

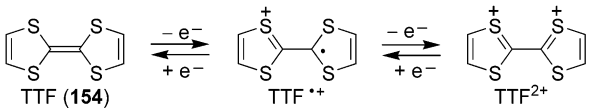

8. Extended Tetrathiafulvalenes (TTFs)

TTF (**154**) is a reversible, two-electron donor (Scheme 16) that has been widely exploited in both advanced materials and supramolecular chemistry.[110] Many structural variations of the parent TTF system have been carried out during the last 30 years, mainly with the aim of developing low temperature organic superconductors.[111] Yet, because of the three reversible redox states of TTF, the possibility for employing TTF in molecular sensors, switches, and devices has also attracted an enormous focus recently.[110a,112] The extension of π-electron conjugation in TTF by a spacer is one important modification.[113]

Acetylenic scaffolding is a powerful tool for constructing extended TTFs based on DEE units. Bis(DEE)-TTF **155**[114] and DEE-TTFs **156**–**158**[115] provide recent examples of such extended TTFs.[116] Compound **155** exhibits a longest wavelength absorption at λ_{max} = 453 nm (ϵ = 61400 $M^{-1}cm^{-1}$), whereas **156** shows an absorption at λ_{max} = 496 nm (67500 $M^{-1}cm^{-1}$). Cyclic voltammetry of **155** reveals a single two-electron oxidation at +0.78 V vs Fc^+/Fc in CH_2Cl_2, which signals that the two dithiafulvene units are so far apart that they behave as independent redox centers. In contrast, **156** is oxidized in two one-electron steps at +0.18 and +0.39 V. These cathodically shifted potentials indicate, interestingly, that **156** is a much stronger donor than **155**. Note that CO_2Me-substituted TTF is oxidized at 0.94 and 1.34 V vs SCE in CH_2Cl_2, corresponding ca. to 0.56 and 0.96 V vs Fc^+/Fc (Chart 24).[117]

Chart 24

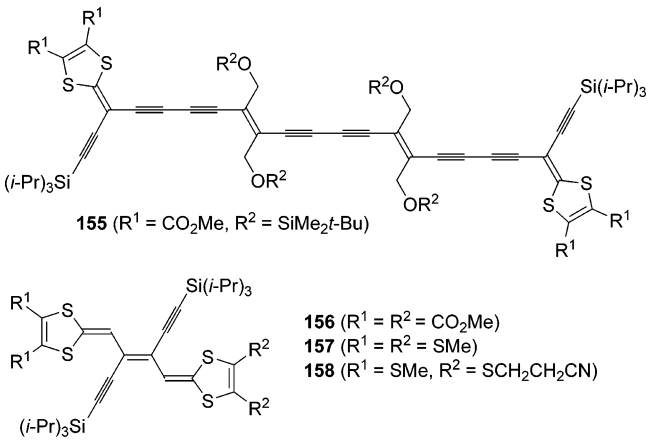

9. Bis(*gem*-DEE)s

The tetraethynyl-*p*-quinodimethane derivatives **107**–**109** described above represent examples of bis(*gem*-DEE)s. We will now focus our attention on other derivatives containing different spacer groups and outer substituents. Thus, Kim and co-workers[118] prepared compounds **159**–**180** and investigated their fluorescence properties. Most of these compounds display two strong emission bands in the visible region. However, the emission wavelength and fluorescence quantum yields are very dependent on the structure. Thus, fluorophores **170** (λ_{em} = 461, 490 nm, ϕ_F = 0.39), **172** (λ_{em} = 473, 498 nm, ϕ_F = 0.49), **173** (λ_{em} = 473, 501 nm, ϕ_F = 0.31), **174** (λ_{em} = 475, 506 nm, ϕ_F = 0.35), and **176** (λ_{em} = 522, 549 nm, ϕ_F = 0.34) show large Stokes shifts relative to those of the less-conjugated fluorophore **180** [λ_{em} = 392 nm, ϕ_F = not detectable (n.d.)], and a substantial increase in fluorescence quantum yield is observed because of the extension of π-conjugation. Similarly, the wavelengths of the absorption and emission maxima of **169** (λ_{em} = 413, 431 nm, ϕ_F = 0.06), which lacks extensive π-conjugation because of the *meta* linkage, are shorter than those of **170**, **172**–**174**, and **176**. The presence of an electron-accepting substituent in the core moiety of bis(*gem*-DEE) **171** (λ_{em} = 560 nm, ϕ_F = n.d.) diminishes its fluorescence drastically when compared with **174**. The incorporation of electron donors, however, in the core moiety in bis(*gem*-DEE) **176** does not affect its fluorescence quantum yield or emission lifetime. These units result in significant red shifts in the absorption and emission wavelength maxima of **176** and a slight increase in emission lifetime, as compared to those of bis(*gem*-DEE) **174**. Incorporation of methyl groups as in **178** at the vinylic positions results in a decrease in fluorescence intensity (λ_{em} = 454, 471 nm, ϕ_F = 0.03). Bis-DEEs **170** and **172**–**174** display similar bright blue emissions and reasonably good quantum yields. Apparently, increasing the length of conjugation in the π-system increases the quantum yield of fluorescence. Very low quantum yields of **175** (n.d.) and **179** (n.d.) are explained by intermolecular stacking interactions even at low concentrations (Chart 25).

10. Dendrimers

π-Conjugated dendrimers based on bis(enediynyl)-benzene units (**181a**–**c**) were prepared by Hwang and Kim.[119] The G1 (generation one) dendrimer **181a** shows an absorption maximum at λ_{max} = 433 nm (ϵ = 22500 M^{-1} cm^{-1}), whereas those of the G2 (**181b**) and G3 (**181c**) derivatives are actually blue-shifted with λ_{max} at 415 (ϵ = 61500 M^{-1} cm^{-1}) and 418 (ϵ = 86000 M^{-1} cm^{-1}) nm, respectively. Blue shifts in the emission maxima of G2 and G3 were also observed. The three generations feature strong bluish-green dual fluorescence with emission maxima at 497 (**181a**), 468 (**181b**), and 469 (**181c**) nm. However, the quantum efficiencies are considerably stronger for the larger generation dendrimer, ϕ = 0.38 (**181a**), 0.79 (**181b**), and 0.80 (**181c**) (Chart 26).

The related dendrimers **182** and **183** containing peripheral *p*-dodecoxyphenyl substituents were reported by Neckers and co-workers.[120] The absorption and emission maxima of **182** (λ_{max}^{abs} = 428 nm, λ_{max}^{em} = 485 nm) are red shifted relative to those of **183** (λ_{max}^{abs} = 347 nm, λ_{max}^{em} = 428 nm), which is a consequence of the better conjugation via a para linkage at the central benzene core than a meta linkage. Moreover, the fluorescence quantum yield is significantly higher for **182** (ϕ = 0.51) than for **183** (ϕ = 0.35).

Chart 25

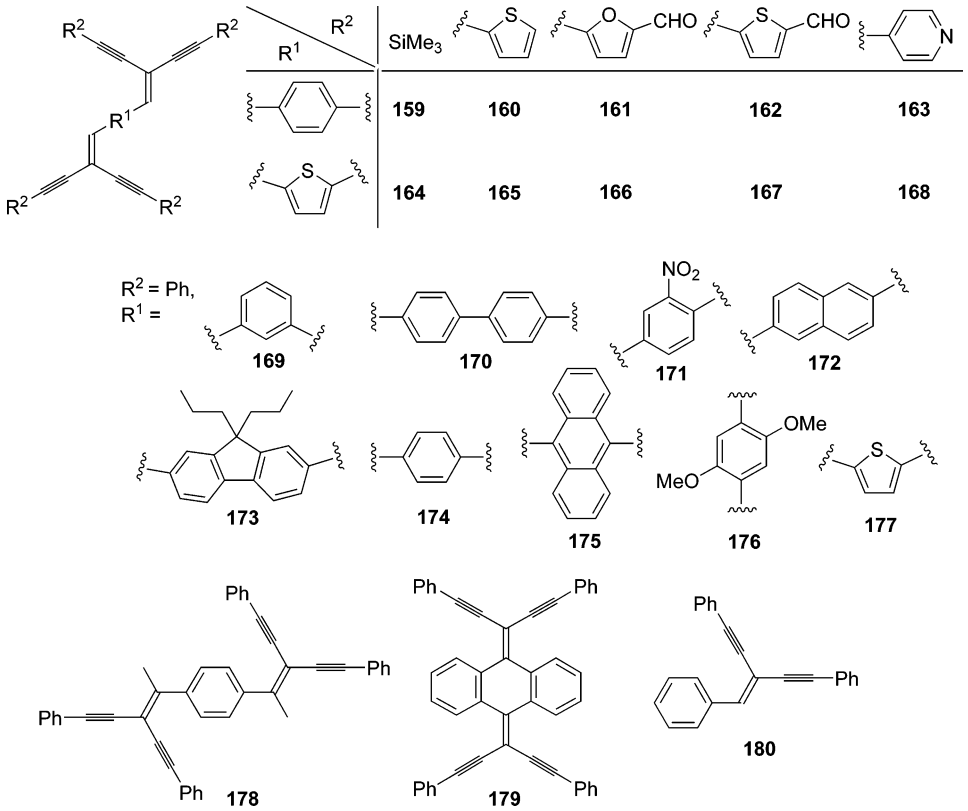

Chart 26

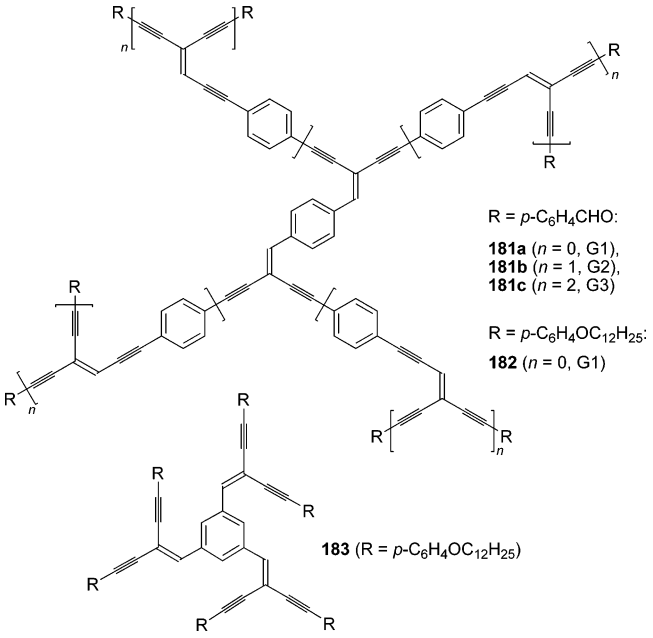

11. Polyelectrochromic *gem*-DEE Systems

Ito et al.[121] recently prepared the novel polyelectrochromic systems **184**−**188** based on *gem*-DEEs about a central core and outer azulenyl groups. The cyclic voltammograms of **184** and **185** are characterized by two one-step, two-electron reduction waves. The first cathodic peaks correspond to the reduction generating the closed shell dianions. The second peaks are attributable to the formation of a tetraanionic species. Spectroelectrochemical measurements revealed a new absorption band in the near-IR region for the dianions of **184** and **185** (λ_{max} 844 and 885 nm, respectively), which is attributed to a cyanine type structure (Scheme 17). Accordingly, the color of the solutions of **184** (orange) and **185** (red)

Scheme 17. Reversible Reductions of 184[121]

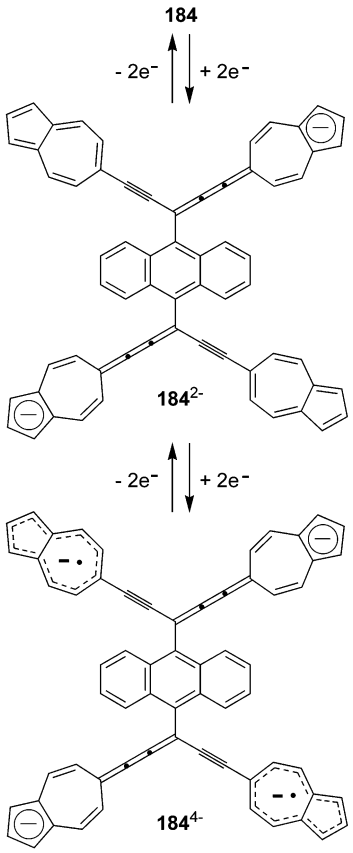

gradually changed to deep green during the electrochemical reduction. On further reduction of **184**, the band in the near-IR region gradually decreased. Instead, a new absorption band at λ_{max} 752 nm arose and the solution turned light blue. The electrochemical reduction of the azulene-containing fluorenes **186** and **187** reveals three reversible single-electron transfers, ultimately generating trianionic species (Chart 27).

Chart 27

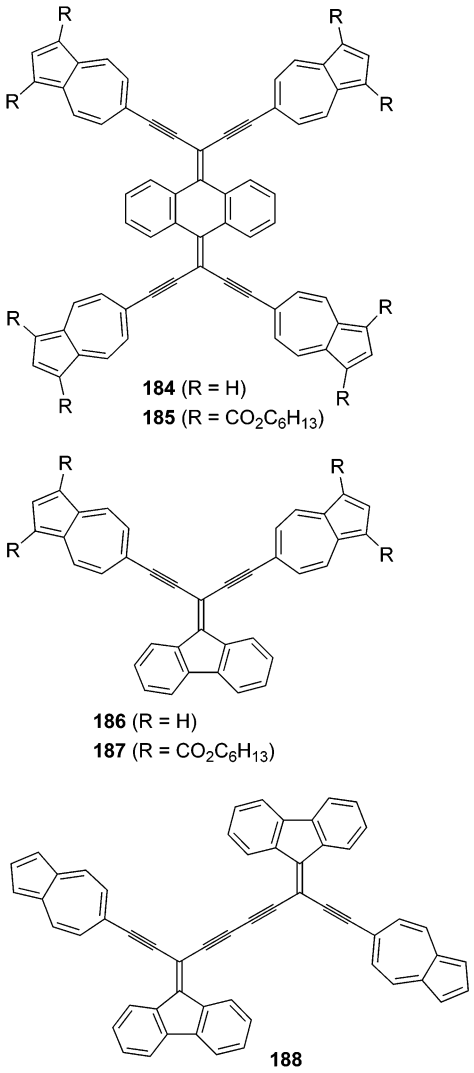

12. Cyclic Structures: Dehydroannulenes and Expanded Radialenes

DEEs and TEEs have been incorporated into a wide variety of cyclic molecules containing all-carbon cores, such as dehydroannulenes and expanded radialenes. Mixed cycles hereof have been deemed radiaannulenes. Moreover, it deserves mention that DEE moeities were employed in one of the first tether-directed syntheses of a C_{60} bis-adduct, i.e., a macrocycle containing both DEE and C_{60} moieties. For work on C_{60}/DEE scaffolding, we shall go in no further detail but refer the reader to ref 18a.

12.1. Dehydroannulenes

Annulenes are cyclic oligoenes formally containing alternating single and double bonds (vinylogs of benzene) and were first prepared by Sondheimer et al.[122] Upon formal insertion of triple bonds between each pair of double bonds, expanded annulenes or dehydroannulenes are obtained.[6,37,38,77,123] Examples are 1,5,9-tridehydro[12]annulene **189**,[123b,c] 1,3,7,9,-13,15-hexadehydro[18]annulene **51**,[6,38] and 1,3,7,9,-13,15,19,21-octadehydro[24]annulene **190**.[77] The ^{1}H NMR spectrum of [12]annulene **189** provided experimental evidence for the existence of a paramagnetic ring current and the assignment of antiaromaticity to this $4n$ π-electron system, whereas a diatropic ring current exists in aromatic [18]annulene **51** ($4n + 2$ π-electron system). The presence of a planar perimeter in **51** is supported by the electronic absorption spectrum, which shows a characteristic vibrational structure with strong absorptions between $\lambda = 300$ and 350 nm and an end absorption around 420 nm. The longest wavelength absorption maxima of the three dehydroannulenes are listed in Table 8. The

Table 8. Longest Wavelength Absorption Maxima (λ_{max}) and Corresponding Energies (E_{max}) of Dehydroannulenes[6,60b,77,123b,126]

compd	solvent	λ_{max} (nm) [ϵ (M^{-1} cm^{-1})]	E_{max} (eV)
189	isooctane	457 (177)	2.71
51	cyclohexane	405 (sh, 790)	3.06
190	ether	352 (45100)	3.52
196a	pentane	614 (270)	2.02
196b	pentane	453 (56000)	2.74
197a	chloroform	566 (sh, 20600)	2.19
197b	chloroform	533 (sh, 99000)	2.33

[12]annulene **189** exhibits intense absorptions at λ_{max} = 239 and 247.5 nm and a low intensity maximum at 457 nm. The [24]annulene **190** is formally derived from cyclooctatetraene by insertion of four butadiynediyl units and, like this compound, appears to be nonplanar. This follows from the general similarity of the electronic spectrum to that of bis-DEE **63** and very similar longest wavelength absorption maxima: λ_{max} = 347 nm for **63** and λ_{max} = 352 nm for **190**. Moreover, the position of the single resonance in the ^{1}H NMR spectrum is not shifted upfield for **190** as compared with linear models. However, electron spin resonance studies suggest the generation of a planar structure (simple spectrum requiring high symmetry) upon reduction of **190** to the monoanion.[77] The dianion obtained by further reduction exhibits a proton chemical shift at a lower field than expected for a localized system having two excess electrons, which is an indication of a planar structure for the dianion of **190** as well (Chart 28).

Chart 28

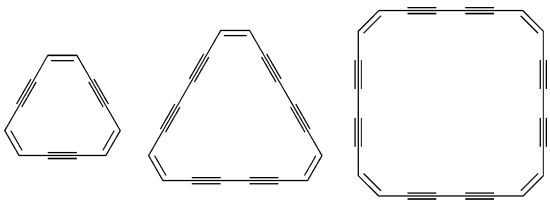

Compound **189** has a melting point of 95−95.5 °C. It is extremely reactive with oxygen, both in solutions

and as a crystalline solid. However, in the absence of oxygen, it is stable. Compound **51** is highly unstable in the crystalline state; it decomposes within a few hours at room temperature and explodes at ca. 85 °C. Compound **190** has an explosion point of ca. 130 °C.

The dodecadehydro[18]annulene **191** (Scheme 18) was prepared by Diederich et al.[124] This annulene

Scheme 18. Formation of Cyclo[18]carbon upon Laser-Induced Retro-Diels–Alder Reaction of Dodecadehydro[18]annulene 191[124]

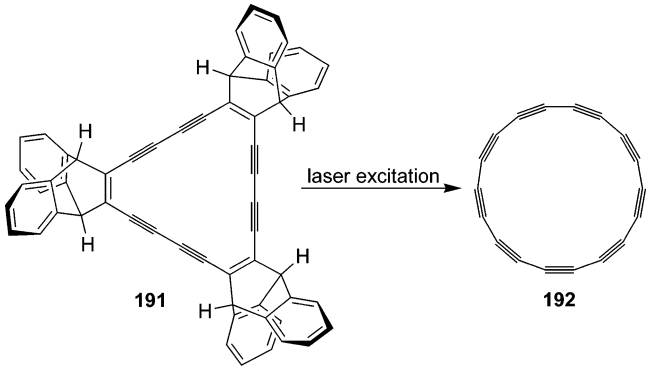

serves as a precursor to cyclo[18]carbon **192**, since it can lose three anthracene units in a retro-Diels–Alder reaction upon laser pyrolysis. Compound **191** is aromatic according to ^{1}H NMR criteria and is among the most stable [18]annulenes ever reported. Thus, it can be heated to 250 °C in the solid state (sealed tube) without decomposition and is perfectly stable to air.

The cycles **193a–c** and **194a–c** represent examples of cyclobutenodehydroannulenes prepared by Diederich and co-workers[125] by oxidative cyclization of enediyne precursors. The formation of a mixture of macrocyclic oligomers (**193a–c**) obtained in the oxidative cyclization differs strikingly from the exclusive formation of [18]annulene **51** in the cyclization of (*Z*)-**1**, as reported by Okamura and Sondheimer.[6] All three compounds are kinetically quite stable, and crystals can be kept for weeks at room temperature and ambient atmosphere without noticeable decomposition. Similarly, the cyclic compounds **194a–c** were obtained upon oxidative cyclization, as mixtures of diastereoisomers. In this series, the trimer is slightly unstable (Chart 29).

(*Z*)-TEEs were employed as building blocks for the construction of stable, perethynylated dehydroannulenes **195a**,**b**,[126] **196a**,**b**,[126] and **197a**,**b**.[60b,127b] Both **196a** and **197b** were found to have planar cores according to X-ray crystallographic analysis, and their electronic absorption bands show considerable vibrational fine structure. In agreement with its antiaromaticity, the per(silylethynylated) dehydro[12]annulene **196a** featured a much lower HOMO–LUMO gap (2.02 eV, Table 8) than the corresponding aromatic dehydro[18]annulene **196b** (2.74 eV), with weak bands appearing between 490 and 620 nm, leading to a characteristic magenta-purple color. In the donor-substituted antiaromatic dehydro[12]annulene **197a**, these weak bands are now completely overlapped by an intramolecular CT transition with

Chart 29

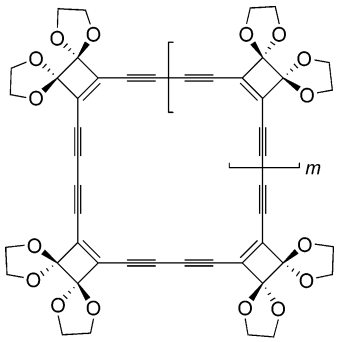

193a-c (*m* = 0,1,2)

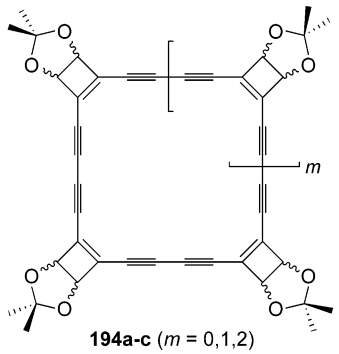

194a-c (*m* = 0,1,2)

absorption maximum λ_{max} = 518 nm (2.39 eV, ϵ = 35100 M^{-1} cm^{-1}) and end absorption around 700 nm (1.77 eV) (shoulder at 566 nm, Table 8). The dehydro[18]annulene **197b** exhibits a CT absorption band also at 518 nm, but with a much higher intensity (ϵ = 105200 M^{-1} cm^{-1}), and a shoulder at 533 nm. Clearly, both **197a** and **197b** are capable of mediating π-electron donor–acceptor conjugation in a similar fashion, but it is somewhat surprising that the intensity of the CT band of **197a** is significantly weaker than that of **197b**, even when the smaller number of donor–acceptor conjugation paths is taken into account. One might have expected the CT to be more efficient in the [12]annulene, as the uptake of electrons reduces the antiaromaticity, whereas, in the case of [18]annulene, the uptake of electrons is accompanied by loss of aromaticity (Chart 30).

Chart 30

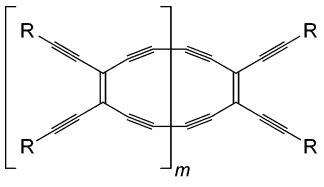

195a,b (R = $SiMe_3$, *m* = 1,2)
196a,b (R = $Si(i\text{-}Pr)_3$, *m* = 1,2)
197a,b (R = $p\text{-}C_6H_4NMe_2$, *m* = 1,2)

12.2. Expanded Radialenes

Radialenes are a series of all-methylidene-substituted cycloalkanes of molecular formula C_nH_n.[128] Upon formal insertion of ethynediyl or buta-1,3-diynediyl moieties into the cyclic framework, the carbon-rich homologous series of expanded radialenes with the molecular formulas $C_{2n}H_n$ and $C_{3n}H_n$, respectively, are obtained.

The perethynylated [3]radialenes **198** and **199**, consisting of three *gem*-DEE units, were prepared by Diederich and co-workers.[129] The electronic absorption spectrum of **198** extends to an end absorption around 620 nm with the longest wavelength band at $\lambda_{max} = 567$ nm (Table 9). This band is thus remarkably red shifted relative to that of *gem*-DEE **24a** (246.8 nm). X-ray crystallographic analysis reveals that the perethynylated core is nearly planar with a maximum deviation of 0.046 Å out of the best plane. The radialene is readily reduced in two reversible one-electron transfers occurring at −0.52 and −1.09 V in CH_2Cl_2 (vs Ag/AgCl). The easy electron uptake was recently explained in a theoretical study by an aromaticity enhancement upon reduction (Chart 31).[130]

Table 9. Longest Wavelength Absorption Maxima (λ_{max}) and Corresponding Energies (E_{max}) of Radialenes[66,81,96b,126b,129,131]

compd	solvent	λ_{max} (nm) [ϵ (M^{-1} cm^{-1})]	E_{max} (eV)
198	hexane	567 (41000)	2.19
200a	hexane	451 (77200)	2.75
200b	hexane	441 (107800)	2.81
200c	hexane	446 (77700)	2.78
201a	chloroform	505 (sh, 51100)	2.46
201b	chloroform	499 (sh, 60200)	2.48
201c	chloroform	508 (sh, 84600)	2.44
202a	chloroform	646 (171000)	1.92
202b	chloroform	636 (sh, 114000)	1.95
202c	chloroform	630 (sh, 64400)	1.97
202d	chloroform	609 (sh, 77600)	2.04
204	chloroform	286 (53600)	4.34
205	chloroform	336 (13200)	3.69
206	chloroform	336 (6200)	3.69
207a	chloroform	333 (26000)	4.73
207b	chloroform	331 (27800)	3.75
207c	chloroform	329 (29500)	3.77
207d	chloroform	329 (30500)	3.77
207e	chloroform	328 (24500)	3.78

Chart 31

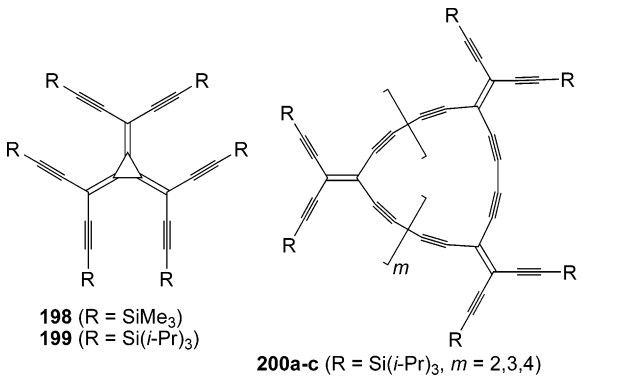

Geminally substituted TEEs are perfect building blocks for the construction of perethynylated expanded radialenes. The macrocycles **200a**−**c**, **201a**−**c**, and **202a**−**d** represent examples hereof.[81,96b,126b] The absorption spectra of the expanded radialenes were compared to those of their related TEE dimers, which serve as models for the longest linearly conjugated π-electron fragment in the macrocycles. Within each radialene series, the optical end absorption remained almost constant, and hence not dependent on the ring size. The donor-substituted radialenes **201a**−**c** and **202a**−**d** displayed strong CT transitions (Table 9), with end absorptions extending to 575 and 750 nm, respectively. The electron-accepting ability of the cyclic core was also evidenced electrochemically. The radialenes exhibit a strong ability to accommodate electrons upon reduction. Thus, in all three series, the first reduction occurred at anodically shifted potentials relative to the reference TEE dimers; the shifts were observed as follows: +170−440 mV for **200a**−**c** relative to **87**, +210−330 mV for **201a**,**b** relative to **203**,[81] and +240−320 mV for **202a**−**c** relative to **88**. Thus, the radical anions of expanded radialenes are very stable, in particularly those of the expanded [3]- and [4]-radialenes, which might be due to some gain of aromaticity upon reduction (Chart 32).[130]

Chart 32

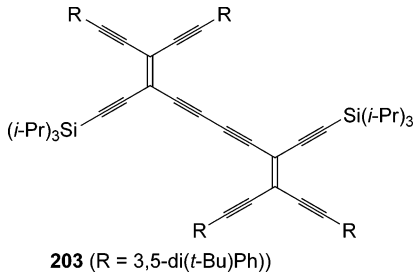

X-ray crystal structure analysis of the expanded [6]radialene **201b** reveals that the cyclic core adopts a nonplanar, "chairlike" conformation, with an average torsional angle of 57.2°.[81] Each buta-1,3-diynediyl moiety only deviates slightly from linearity. Thus, the corresponding bond angles vary from 174 to 180°. The six individual TEE units are almost planar, with deviations up to only 0.03 Å from the mean plane.

The ethynediyl-expanded radialene **204**, hybrid radialenes **205** and **206**, and cyclic bis-DEEs **207a**−**e** were prepared by Tykwinski and co-workers.[66,131] The absorption spectrum of [6]radialene **204** is conveniently compared to that of rotationally unencumbered, acyclic **208** (expanded dendralene). Compound **208** shows two low energy absorptions at $\lambda_{max} = 283$ nm and about 305 nm for *cisoid* and *transoid* ene-yne-ene orientations, respectively. Structurally rigid radialene **204** shows only one major low energy absorption, at 286 nm, which is ascribed to the *cisoid* ene-yne-ene conformation in this molecule. The UV/vis spectra suggest that homoconjugation contributes little to the overall π-electron delocalization in **204**, since this radialene has similar absorption characteristics to acyclic **208**.[131a] The similar absorption energies predict virtually the same extent of overall π-delocalization in the two molecules as a sum of linear and cross-conjugation (Charts 33 and 34).

The major electronic absorption of hybrid radialene **205** is at $\lambda_{max} = 293$ nm and is hence slightly red shifted (by 10 nm) relative to the same absorption in **204**.[131a] This red shift is possibly the result of increased planarity in **205**. The absorption spectrum has an additional low energy band around $\lambda_{max} = 336$

Chart 33

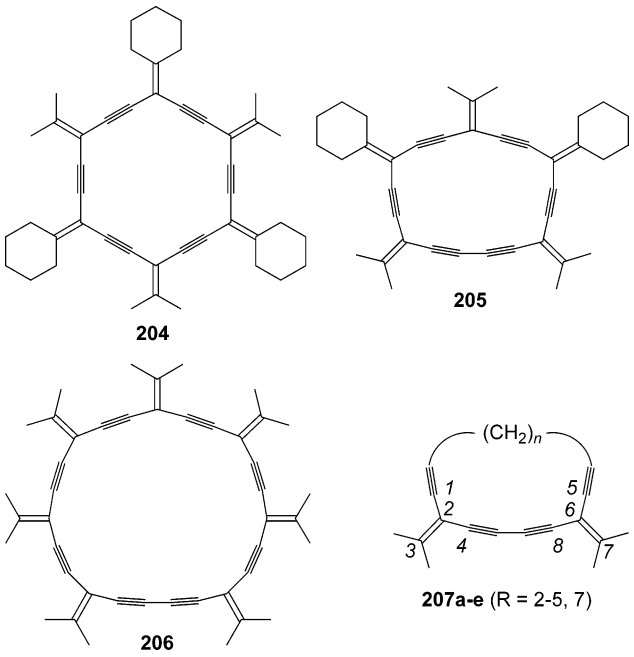

Chart 34

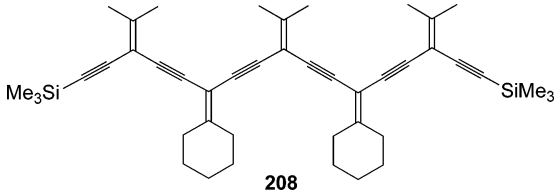

nm. For **206**, an intense absorption is seen at λ_{max} = 280 nm and a weaker at 336 nm.[66]

Tykwinski and co-workers[131b] investigated the characteristics of enyne macrocycles **207a**−**e** as a function of ring strain. These molecules can also be regarded as cyclic expanded dendralenes. X-ray crystallographic analyses reveal that the planarity of the conjugated portion of the macrocycles in the solid state varies considerably and is not associated directly with decreasing ring size. The angles between the planes C1−C2−C3−C4 and C5−C6−C7−C8 provide an estimate of the planarity. For the most conformationally flexible macrocycle **207e**, with two crystallographic independent molecules A and B, the twist angle is greatest for molecule A at 22.2(2)° and somewhat smaller for molecule B at 12.3(7)°. The twist is approximately equal for **207c** and **207d** at 3.36(19) and 2.82(13)°, respectively. Macrocycle **207b** is quite distorted out of planarity as a result of the small alkyl bridge in the molecule, with an angle of 8.22(16)°. Despite the considerably increased ring strain of **207a**, the twist angles at 7.0(2) and 6.2(2)° for the two crystallographically independent molecules A and B, respectively, are greater than those angles in either **207c** or **207d**. Increased twist and bond strain in the conjugated portion of **207a** is necessary for the accommodation of a small ethanediyl bridge and the two *exo*-methylene moieties in this macrocycle. The longest wavelength absorption maxima for the five cycles are collected in Table 9.

Tobe et al.[132] prepared the expanded radialenes **209a**−**d** with bicyclo[4.3.1]decatriene units.[133] In

Scheme 19. Formation of Cyclo[*n*]carbons in Negative-Mode Laser Desorption Time-of-Flight Mass Spectrometry from Expanded Radialenes 209a−d[132]

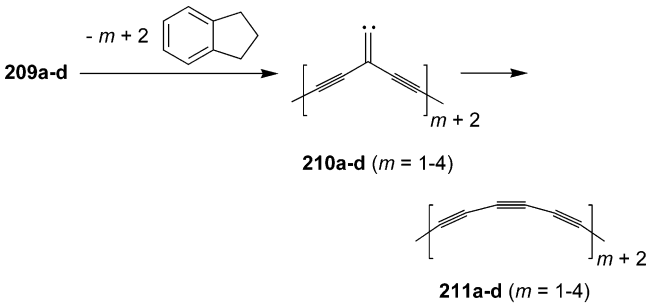

negative mode laser desorption time-of-flight mass spectra, these expanded radialenes exhibited peaks assignable to the corresponding cyclo[*n*]carbon anions (n = 18, 24, 30, and 36) formed by the stepwise loss of the aromatic indane fragments (Scheme 19) followed by isomerization of the resulting vinylidenes (**210a**−**d**) (Chart 35).

Chart 35

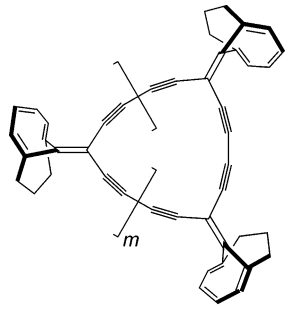

12.3. Radiaannulenes

Recently, the new family of all-C macrocycles **212**−**218** was reported.[127] These molecules can, from a structural viewpoint, be regarded as hybrids between dehydroannulenes and expanded radialenes and were therefore called radiaannulenes. The X-ray crystal structure of radiaannulene **212** shows a virtually planar macrocyclic framework with a mean out-of-plane deviation of 0.040 Å and a maximum deviation of 0.091 Å. Strain in the 16-membered ring is expressed by bending of the three buta-1,3-diynediyl moieties with C≡C−C(sp) angles as low as 169.2° and by a deviation of the C(sp)−C(sp^2)−C(sp) angles at the exocyclic ethylene units from ideally 120° to ca. 111°. Most strain occurs, however, at the macrocyclic C≡C−C(sp^2) angles with a bending from ideally 180° to ca. 164° (Chart 36).

The anilino-substituted monocyclic perethynylated radiaannulenes also display intense intramolecular CT bands in chloroform that disappear upon acidification, and similar UV/vis spectra are obtained for the protonated compounds. Position and intensity of the CT band are affected by the number of peripheral donor groups. Thus, the CT band of dianilino-substituted **212** is rather weak (λ_{max} = 588 nm, ϵ = 31900 M^{-1} cm^{-1}) and detectable only as a shoulder. In contrast, hexaanilino-substituted **213** features a

Chart 36

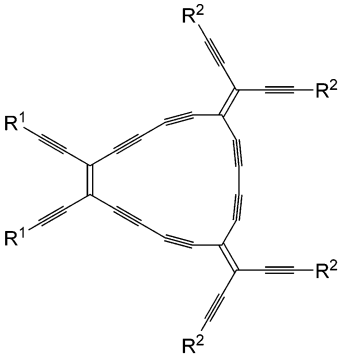

212 (R^1 = *p*-$C_6H_4NMe_2$, R^2 = Ph)
213 (R^1 = *p*-$C_6H_4NMe_2$, R^2 = *p*-$C_6H_4N(C_6H_{13})_2$)
214 (R^1 = *p*-$C_6H_4NMe_2$, R^2 = *p*-$C_6H_4NO_2$)
215 (R^1 = *p*-$C_6H_4NO_2$, R^2 = *p*-$C_6H_4N(C_6H_{13})_2$)

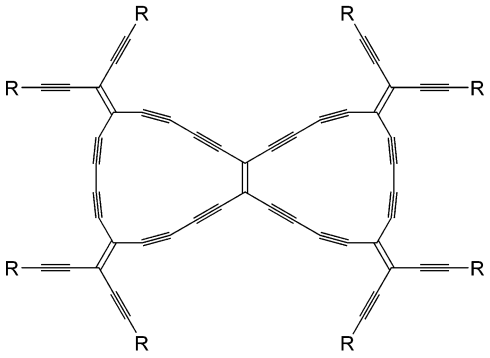

216 (R = Ph)
217 (R = 2,5-di(*t*-Bu)Ph)
218 (R = *p*-$C_6H_4N(C_6H_{13})_2$)

split CT band (λ_{max} = 521 nm, ϵ = 106100 M^{-1} cm^{-1} and λ_{max} = 615 nm, ϵ = 99900 M^{-1} cm^{-1}), being much more intense and bathochromically shifted. The end absorptions of both compounds, however, are nearly identical (around 700 nm, 1.77 eV). Introducing two 4-nitrophenyl acceptor groups in **215**, while keeping four peripheral anilino donor groups, does not affect the position of the longest wavelength maximum of the split CT band as compared with hexa-donor-substituted **213**. The end absorption, however, shifts substantially to ca. 800 nm (1.55 eV) in **215**. The intramolecular CT can be further assessed by determining the quinoid character of the anilino ring. On the basis of the bond lengths from the X-ray crystal structure analysis, an average value δr = 0.0245 is calculated for the two anilino groups of **212**, indicating considerable quinoid character of the rings and signaling the existence of intramolecular CT in the ground state.

The compounds **219**−**225** served as precursors for the radiaannulenes.[127] A comparison of the UV/vis spectra of acyclic TEE trimer **220** and radiaannulene **213** reveals a significant difference. On one hand, the longest linear π-conjugation pathways in both compounds are identical, and the optical end absorptions occur at similar wavelengths (around 700 nm, 1.77 eV). On the other, however, the lowest energy band with CT character in acyclic **220** appears at λ_{max} = 486 nm (ϵ = 98800 M^{-1} cm^{-1}), whereas hexaanilino-substituted **213** features a split CT band at λ_{max} = 521 and 615 nm. Hence, the fact that the acetylenic core of **213** is a better electron acceptor (as expressed by the bathochromic shift of the CT band) is a special feature of the macrocyclic scaffold. A similar effect was also observed for the anilino-substituted expanded radialene **202a**, which displays a pronounced macrocyclic π-conjugation effect when compared with acyclic TEE dimer **88** possessing the same longest linear π-conjugation pathway (Chart 37).[81]

Chart 37

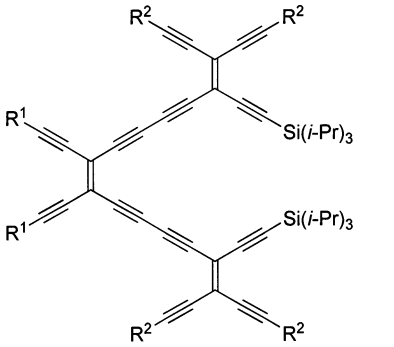

219 (R^1 = *p*-$C_6H_4NMe_2$, R^2 = Ph)
220 (R^1 = *p*-$C_6H_4NMe_2$, R^2 = *p*-$C_6H_4N(C_6H_{13})_2$)
221 (R^1 = *p*-$C_6H_4NMe_2$, R^2 = *p*-$C_6H_4NO_2$)
222 (R^1 = *p*-$C_6H_4NO_2$, R^2 = *p*-$C_6H_4N(C_6H_{13})_2$)

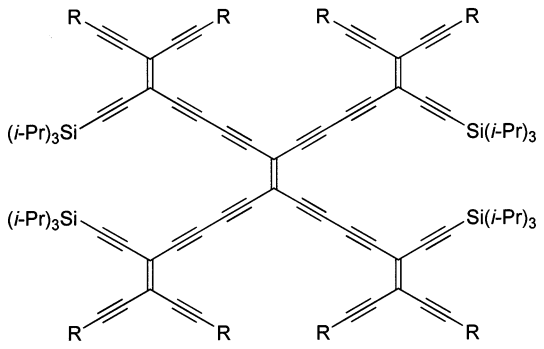

223 (R = Ph)
224 (R = 2,5-di(*t*-Bu)Ph)
225 (R = *p*-$C_6H_4N(C_6H_{13})_2$)

Dehydroannulene **197b**, expanded radialene **202a**, and radiaannulene **213** are all macrocyclic TEE trimers with the same number of peripheral anilino donor groups. Nonetheless, their UV/vis spectra display profound differences. The longest wavelength CT absorption shifts bathochromically from λ_{max} = 518 nm in **197b** (with a shoulder at 533 nm) to 615 nm in **213** and to 646 nm in **202a**, while at the same time, the optical end absorption also shifts from around 700 nm (in **197b** and **213**) to around 750 nm (in **202a**). Furthermore, the exceptionally high molar extinction coefficient of the CT band of radialene **202a** (λ_{max} = 646 nm, ϵ = 171100 M^{-1} cm^{-1}, Table 9), when compared with **197b**, is noteworthy. Clearly, the capability of macrocyclic TEE scaffolds to mediate CT interactions depends much on the arrangement of the TEE moieties in the macrocyclic all-carbon perimeter.

Bicyclic radiaannulene **218** with its electron-accepting C_{50} core features the most intense and the

most bathochromically shifted CT absorptions of all macrocyclic TEE derivatives prepared so far. Its UV/vis spectrum displays two intense maxima at λ_{max} = 558 nm (ϵ = 176700 M^{-1} cm^{-1}) and λ_{max} = 698 nm (ϵ = 85900 M^{-1} cm^{-1}). The end absorption reaches 850 nm (1.46 eV), which is the lowest energy one known for TEE oligomers. Even expanded [5]- and [6]radialenes with C_{50} and C_{60} cores and 10 or 12 peripheral anilino groups, respectively, do not feature such low energy CT transitions and optical end absorptions. This observation is interpreted as strong evidence for particularly efficient electronic communication within the bicyclic core of **218**.

The bicyclic octaanilino-substituted radiaannulene **218** shows three well-separated, one-electron reduction steps at −0.99, −1.36, and −1.78 V vs Fc^+/Fc in THF. Remarkably, these potentials are less negative than those measured for hexaanilino-substituted macrocycles, which already indicates that the bicyclic all-C core has exceptional electron−acceptor properties. Two irreversible oxidation peaks for the anilino groups are observed at +0.48 and +0.57 V. Bicyclic radiaannulene **217**, lacking anilino donor groups, displays an extremely low first reduction potential at −0.83 V. This is the lowest value (i.e., less negative, relative to Fc^+/Fc) observed for any macrocyclic TEE oligomer and is even lower than the first reduction potential of buckminsterfullerene C_{60} (−1.02 V under comparable conditions[69,134]), which is considered as a very good electron acceptor.

12.4. Benzo-Fused and Other Annelated Dehydroannulenes

Benzannelated dehydroannulenes have attracted for decades the interest of several groups with respect to the extent of delocalization in the macrocyclic ring.[135] In other words, the question was raised and answered to what extent annulenoid macrocyclic conjugation can compete with the strong benzenoid conjugation when the macrocycle is fused to benzene, naphthalene, and other benzenoid aromatic ring systems.

We shall limit our coverage of this extensive topic to some recent studies of benzannelated octadehydro[14]annulenes. Thus, these annulenes were prepared with the prospect to elucidate the degree of aromaticity in comparison to the parent octadehydroannulene **226**. Compounds **227**−**231** provide examples hereof.[136,137] Table 10 lists the alkene proton chemical shifts for these compounds and the 1,2-dihydro analogue **62** where the cyclic conjugation is broken by an ethanediyl bridge. It transpires that the alkene protons of **226** are significantly downfield shifted relative to those of **62**, which signals the presence of a diatropic ring current. Upon benzannelation, the alkene protons shift upfield. The shift becomes more and more significant as the number of fused benzene rings increases from one (**227** and **228**) to two (**229** and **230**). Thus, benzannelation reduces aromaticity in the annulene circuit, a finding that confirms the pioneering work by Staab and co-workers on other benzannelated dehydroannulenes.[135a−c,e] Studies of the thieno[14]annulenes **232** and **233** also provide useful information. Thus, from NMR spectroscopy, it appears that the thiophene ring in **232** retains more of its benzenoid ring current as compared to a related acyclic analogue than did the thiophene ring in **233**. In **233**, the increased double bond character at the site of fusion results in an increase in the [14]-annulenic circuit in comparison to that in **232**. Thus, the resonances of each of the alkene protons of **233** (δ = 7.60, 7.58, 7.02, and 6.97 ppm) appear more downfield than those of **232** (δ = 6.93 and 6.32 ppm) with a less pronounced macrocyclic diatropicity (Chart 38).

Table 10. Alkene Proton Chemical Shifts (ppm)[a] of Dehydro[14]annulenes[136]

proton[b]	226	227	228	229	230	62
H1	7.77		7.03		6.72	
H2	7.77		7.16		6.72	
H11	7.39	6.73	6.74	6.37		5.79
H12	7.92	7.41	7.24	7.01		6.17

[a] Solvent: CD_2Cl_2. [b] For numbering, see Chart 38.

Chart 38

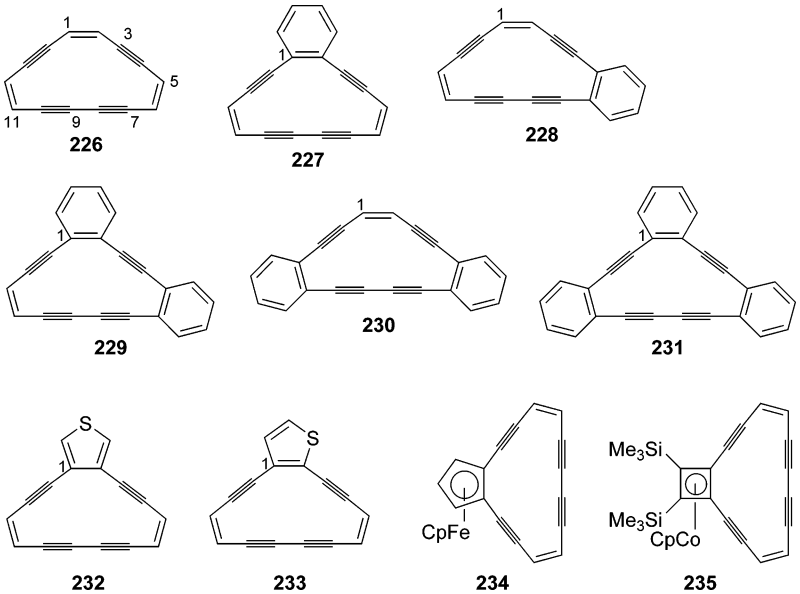

The fusion of [14]dehydroannulene to any cyclic π-system offers the opportunity to elucidate the (relative) aromaticity of the latter, such as of ferrocene in comparison to benzene. Bunz and co-workers[138] studied the ferrocene-based dehydro[14]-annulene **234**. The alkene protons in the annulene ring appear at δ 6.75 and 6.21 ppm, which is upfield shifted relative to those of **227**. Consequently, a benzene ring disturbs the aromaticity of the fused dehydro[14]annulene less than a ferrocene ring. In other words, ferrocene is more aromatic than benzene by this measure. Using again the alkene protons in the dehydroannulene ring as sensors, the aromaticity of CpCo-complexed cyclobutadiene was elucidated in a study on molecule **235**.[138b,c] The alkene proton chemical shifts appear at δ 6.52 and 6.18 ppm, and according to the applied criterion, CpCo-complexed cyclobutadiene is accordingly more aromatic than both ferrocene and benzene.

Srinivasan et al.[139] prepared the [6.6]metacyclophane **236** with DEE bridges. X-ray crystallographic analysis reveals that the structure is nearly planar. In the ^{1}H NMR spectrum, the intra-annular protons appear as a singlet at δ 7.82 ppm, that is, more deshielded than the rest of the aromatic protons, which resonate at δ 7.15 and 7.4 ppm. The alkene protons appear as a singlet at δ 6.05 ppm (Chart 39).

Chart 39

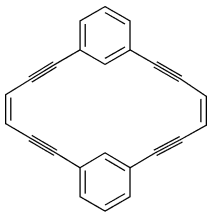

236

Hopf, Haley, and co-workers[140] synthesized [2.2]-paracyclophane **237** with an additional bis-(*Z*)-DEE bridge connecting the two benzene rings. Comparison of the electronic absorption spectrum to that of **227** and related acyclic counterparts reveals the presence of "global" transannular delocalization between the two aromatic decks (Chart 40).

Chart 40

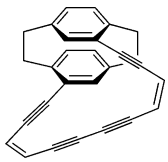

237

13. Cages

Much work has been devoted to the synthesis of carbon-rich cages as precursors for buckminsterfullerene C_{60} and three-dimensional carbon networks.[4,141] The cages **238** and **239** contain (*Z*)-DEE linkages with labile substituents.[142] Thus, exhaustive decarbonylation of **238** or elimination of indane fragments in a retro-[2+2]-cyclization from **239** can provide access to macrocycle **240** ($C_{60}H_6$). In laser desorption mass spectra of **238** and **239**, ions corresponding to $C_{60}H_6^{\bullet-}$ were indeed observed. Moreover, base peaks for $C_{60}^{\bullet-}$ ions were observed with associated fragment ions resulting from the loss of C_2 units ($C_{58}^{\bullet-}$, $C_{56}^{\bullet-}$), which indicates a likely fullerene structure for the ions corresponding to C_{60} and the involvement of **240** in their formation by a polyyne

Chart 41

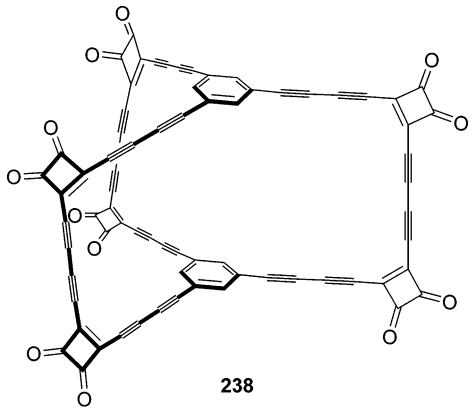

238

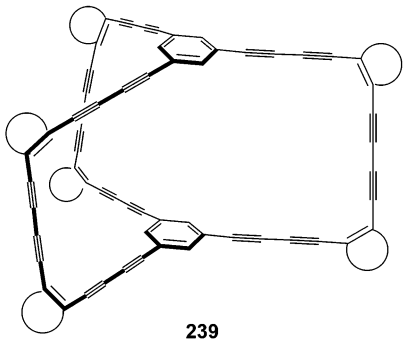

239

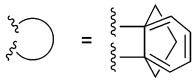

Chart 42

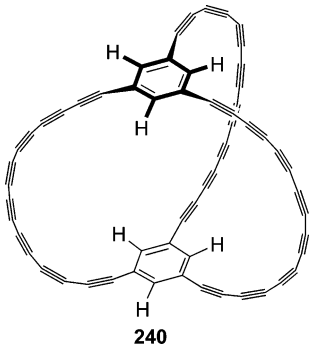

240

Chart 43

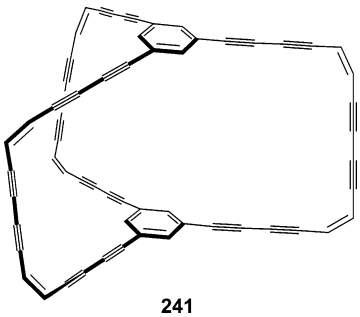

241

Scheme 20. Generation of Corannulenes by Pyrolysis of 242[145]

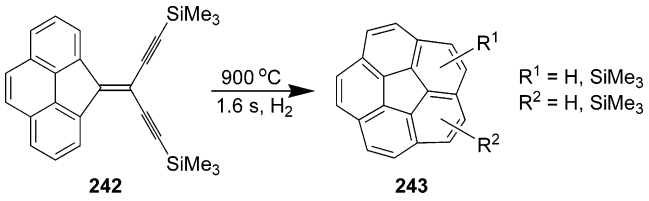

242 243

cyclization mechanism.[143] Rubin et al.[141,144] prepared the cage **241** containing two double bonds in each polyyne bridge. In the ion cyclotron resonance mass spectrum (negative mode) of **241**, partial dehydrogenation down to $C_{60}H_{14}^-$ was observed (Charts 41–43).

Smaller segments of C_{60}, such as corannulene, have also been targeted from DEE-based precursors. Thus, pyrolysis of the geminal DEE **242** provided corannulenes **243**, as well as other polycyclic aromatic hydrocarbons (Scheme 20).[145]

14. DEEs in Supramolecular Chemistry

14.1. Donor–Acceptor Complexes

Perfect planarity makes it possible for tetrakis(phenylethynyl)ethene **31a** to form highly ordered 1:2 stoichiometric donor–acceptor π-complexes in the solid state with electron deficient molecules, such as 2,4,7-trinitrofluoren-9-one **244** and (2,4,7-trinitrofluoren-9-ylidene)malonitrile **245**.[70b,d] The interplanar separation between molecules **31a** and **244** within the complex [**31a**·**244**$_2$] and between **31a** and **245** within the complex [**31a**·**245**$_2$] is 3.39 and 3.33 Å, respectively. In solution, relatively weak 1:1 complexes with each of these two acceptors are formed, with association constants of 7.9 and 31.5 M^{-1}, respectively, at 300 K in $CDCl_3$. Addition of both **244** and **245** to solutions of **31a** resulted in instantaneous color changes—the yellow solution of **31a** turning orange-red on addition of **244** and green on addition of **245**. The observed color change is a result of the appearance of intermolecular CT absorption bands in the visible region of the spectrum with maxima at ca. 520 (shoulder, **31a**·**244**) and 630 (**31a**·**245**) nm. TEE **31a** exhibits an intense blue fluorescence [λ_{max}(emission) = 445 and 470 nm, λ_{exc}(excitation) 410 nm], which is quenched upon addition of **244**. The complexation between **244** and **245** with the related molecules **246**–**249** was also studied.[70d] The following association constants were determined between **244** and **246**–**249**: 1.6, 10.3, 9.9, and 1.6 M^{-1}, respectively. Between **245** and **246**–**249**, the association constants are 3.2, 27.8, 29.6, and 2.2 M^{-1}, respectively (Charts 44 and 45).

Chart 44

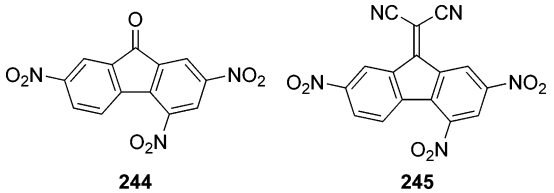

244 245

Chart 45

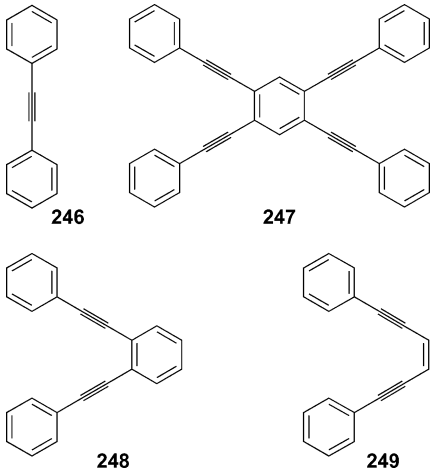

246 247 248 249

14.2. Control of Bergman Cyclization

König and Rütters[146] prepared the bis(crown ether) functionalized DEE **250** and studied the binding of alkali metal ions and how this complexation affected the ability to undergo the Bergman cyclization.[147] On treatment with sodium hexafluorophosphate, two sodium cations are bound, whereas with potassium ions a sandwich complex is formed. The thermal reactivity of the DEE moiety toward cyclization was investigated by differential scanning calorimetry. At lower temperatures, an endothermic process was observed corresponding to melting (**250**, 360 K; **250**·2$NaPF_6$, 390 K; **250**·KPF_6, 420 K). At higher temperatures, an exothermic dip occurred, which may indicate beginning of the cyclization process: at 415 K for **250**, at 430 K for **250**·2$NaPF_6$, and at 442 K for **250**·KPF_6. The energy evolved corresponded to 160, 155, and 162 kJ/mol, respectively. These large values suggest a radical process. The reaction is possibly initiated by the cyclization process forming the diradical, which can then further polymerize with the enediyne moiety of unreacted material. Indeed, the process was found to be irreversible. The increased thermal stability of the metal complexes might originate from their presumable more rigid conformation. Electrostatic repulsion of the sodium ions in **250**·2$NaPF_6$ and the intercalation of the large potassium ion in **250**·KPF_6 could hinder the approach of the triple bonds for cyclization (Chart 46).

14.3. Macrocyclic Ligands

Campbell et al.[148] prepared the macrocycle **251** containing two pyridine coordination sites (Scheme

Chart 46

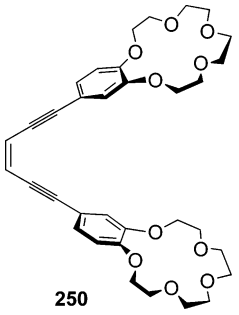

250

Scheme 21. Coordination-Driven Self-Assembly[148]

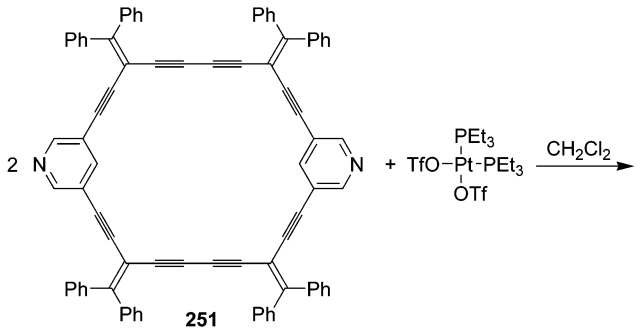

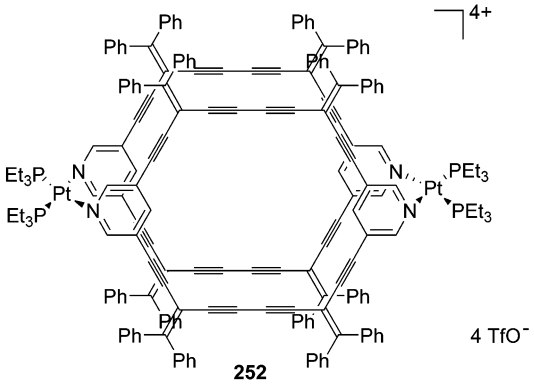

21). Adding this macrocycle to *cis*-[$(TfO)_2Pt(PEt_3)_2$] in CH_2Cl_2 over a period of 2 days gave after slow evaporation of the solvent crystals of the complex **252**. This material was thermally very stable and decomposed only at temperatures higher than 245 °C. X-ray crystallographic analysis reveals that the macrocycle adopts a boatlike conformation in the assembly.

15. Conclusions

Since the pioneering investigations of Sondheimer and Bergman and their co-workers, a large selection of conjugated scaffolds based on the DEE unit has been prepared. The construction of these novel one- and two-dimensional structures, which often extend to multinanometer-sized dimensions, has greatly benefited from two types of synthetic reactions: oxidative acetylenic coupling introduced by Glaser more than 120 years ago and refined by Eglinton[149] and Hay[150] and co-workers in the 1960s and the diverse and efficient Pd-catalyzed cross-coupling protocols invented over the past 30 years. Investigations of DEE-based structures have been rewarding from both fundamental and technological viewpoints. On one hand, they have greatly enhanced our fundamental understanding of π-electron delocalization in linear and cyclic systems. On the other, they have led to new "war heads" for antitumor drugs and produced novel advanced materials with exceptional optoelectronics properties that could find future use in practical devices. The latter perspective is quite realistic in view of the often remarkable thermal (kinetic) stability of DEE-based scaffolds, contrasting their high thermodynamic instability. Both the synthesis and the properties of DEE-based structures have been comprehensively reviewed for the first time in this article, which we hope expresses the clear take-home message that many more exciting findings in this area remain to be made in future research.

16. Acknowledgment

We thank the ETH Research Council as well as the German Fonds der Chemischen Industry for their continuous support of this research. Moreover, the Danish Natural Science and Technical Research Councils are acknowledged for support.

17. References

(1) For reviews of the chemistry and biology of enediyne antitumor agents, see (a) Nicolaou, K. C.; Dai, W.-M. *Angew. Chem., Int. Ed. Engl.* **1991**, *30*, 1387. (b) Maier, M. E. *Synlett* **1995**, 13.
(2) Recent examples: (a) Nielsen, M. B.; Diederich, F. In *Modern Arene Chemistry*; Astruc, D., Ed.; VCH−Wiley: Weinheim, 2002; pp 196−216. (b) Raimundo, J.-M.; Lecomte, S.; Edelmann, M. J.; Concilio, S.; Biaggio, I.; Bosshard, C.; Günter, P.; Diederich, F. *J. Mater. Chem.* **2004**, *14*, 292. (c) Song, J.; Cisar, J. S.; Bertozzi, C. R. *J. Am. Chem. Soc.* **2004**, *126*, 8459.
(3) For recent reviews on acetylenic scaffolding, see (a) Nielsen, M. B.; Diederich, F. *Synlett* **2002**, 544. (b) Nielsen, M. B.; Diederich, F. *Chem. Rec.* **2002**, *2*, 189.
(4) Bunz, U. H. F.; Rubin, Y.; Tobe, Y. *Chem. Soc. Rev.* **1999**, *28*, 107.
(5) (a) Salaneck, W. R.; Lundström, I.; Råånby, B. *Conjugated Polymers and Related Materials*; Oxford University Press: Oxford, 1993. (b) Skotheim, T. A.; Elsenbaumer, R. L.; Reynolds, J. R. *Handbook of Conducting Polymers*, 2nd ed.; Marcel Dekker: New York, 1997. (c) Kraft, A.; Grimsdale, A. C.; Holmes, A. B. *Angew. Chem., Int. Ed. Engl.* **1998**, *37*, 402.
(6) Okamura, W. H.; Sondheimer, F. *J. Am. Chem. Soc.* **1967**, *89*, 5991.
(7) Vollhardt, K. P. C.; Bergman, R. G. *J. Am. Chem. Soc.* **1973**, *95*, 7538.
(8) Figeys, H. P.; Gelbcke, M. *B. Soc. Chim. Belg.* **1974**, *9*, 369.
(9) Nuss, J. M.; Murphy, M. M. *Tetrahedron Lett.* **1994**, *35*, 37.
(10) Fisher, I. P.; Lossing, F. P. *J. Am. Chem. Soc.* **1963**, *85*, 1018.
(11) (a) Walker, J. A.; Bitler, S. P.; Wudl, F. *J. Org. Chem.* **1984**, *49*, 4733. (b) Carpita, A.; Rossi, R. *Tetrahedron Lett.* **1986**, *27*, 4351. (c) Alami, M.; Crousse, B.; Linstrumelle, G. *Tetrahedron Lett.* **1995**, *36*, 3687. (d) Uenishi, J.; Kawahama, R.; Yonemitsu, O. *J. Org. Chem.* **1996**, *61*, 5716. (e) Uenishi, J.; Kawahama, R.; Yonemitsu, O. *J. Org. Chem.* **1998**, *63*, 8965. (f) Marino, J. P.; Nguyen, H. N. *J. Org. Chem.* **2002**, *67*, 6841. (g) Takayama, Y.; Delas, C.; Muraoka, K.; Sato, F. *Org. Lett.* **2003**, *5*, 365. (h) Takayama, Y.; Delas, C.; Muraoka, K.; Uemura, M.; Sato, F. *J. Am. Chem. Soc.* **2003**, *125*, 14163. (i) Schreiber, M.; Anthony, J.; Diederich, F.; Spahr, M. E.; Nesper, R.; Hubrich, M.; Bommeli, F.; Degiorgi, L.; Wachter, P.; Kaatz, P.; Bosshard, C.; Günter, P.; Colussi, M.; Suter, U. W.; Boudon, C.; Gisselbrecht, J.-P.; Gross, M. *Adv. Mater.* **1994**, *6*, 786.
(12) (a) Hynd, G.; Jones, G. B.; Plourde, G. W., II; Wright, J. M. *Tetrahedron Lett.* **1999**, *40*, 4481. (b) Jones, G. B.; Wright, J. M.; Plourde, G. W., II; Hynd, G.; Huber, R. S.; Mathews, J. E. *J. Am. Chem. Soc.* **2000**, *122*, 1937.
(13) Blackwell, J. M.; Figueroa, J. S.; Stephens, F. H.; Cummins, C. C. *Organometallics* **2003**, *22*, 3351.
(14) Camacho, D. H.; Saito, S.; Yamamoto, Y. *J. Am. Chem. Soc.* **2002**, *124*, 924.
(15) Böhm-Gössl, T.; Hunsmann, W.; Rohr-Schneider, L.; Schneider, W. M.; Ziegenbein, W. *Chem. Ber.* **1963**, *96*, 4.
(16) Alberts, A. H. *J. Am. Chem. Soc.* **1989**, *111*, 3093.
(17) Gleiter, R.; Merger, R.; Nuber, B. *J. Am. Chem. Soc.* **1992**, *114*, 8921.
(18) (a) Nierengarten, J.-F.; Hermann, A.; Tykwinski, R. R.; Rüttimann, M.; Diederich, F.; Boudon, C.; Gisselbrecht, J.-P.; Gross, M. *Helv. Chim. Acta* **1997**, *80*, 293. (b) Shultz, D. A.; Gwaltney, K. P.; Lee, H. *J. Org. Chem.* **1998**, *63*, 4034. (c) Kaafarani, B. R.; Neckers, D. C. *Tetrahedron Lett.* **2001**, *42*, 4099. (d) Kaafarani, B. R.; Pinkerton, A. A.; Neckers, D. C. *Tetrahedron Lett.* **2001**, *42*, 8137.
(19) (a) Zhao, Y.; Tykwinski, R. R. *J. Am. Chem. Soc.* **1999**, *121*, 458. (b) Zhao, Y.; Slepkov, A. D.; Akoto, C. O.; McDonald, R.; Hegmann, F. A.; Tykwinski, R. R. *Chem. Eur. J.* **2005**, *11*, 321.
(20) (a) Tseng, C. K.; Migliorese, K. G.; Miller, S. I. *Tetrahedron* **1974**, *30*, 377. (b) Livingston, R.; Cox, L.; Odermatt, S.; Diederich, F. *Helv. Chim. Acta* **2002**, *85*, 3052.
(21) Hori, Y.; Noda, K.; Kobayashi, S.; Taniguchi, H. *Tetrahedron Lett.* **1969**, *10*, 3563.
(22) Hauptmann, H. *Tetrahedron* **1976**, *32*, 1293.
(23) Rossi, R.; Carpita, A.; Bigelli, C. *Tetrahedron Lett.* **1985**, *26*, 523.

(24) (a) Hauptmann, H. *Tetrahedron Lett.* **1975**, *16*, 1931. (b) Hauptmann, H. *Angew. Chem., Int. Ed. Engl.* **1975**, *14*, 498.
(25) Tykwinski, R. R.; Diederich, F.; Gramlich, V.; Seiler, P. *Helv. Chim. Acta* **1996**, *79*, 634.
(26) Koentjoro, O. F.; Zuber, P.; Puschmann, H.; Goeta, A. E.; Howard, J. A. K.; Low, P. J. *J. Organomet. Chem.* **2003**, *670*, 178.
(27) (a) Rubin, Y.; Knobler, C. B.; Diederich, F. *Angew. Chem., Int. Ed. Engl.* **1991**, *30*, 698. (b) Anthony, J.; Boldi, A. M.; Rubin, Y.; Hobi, M.; Gramlich, V.; Knobler, C. B.; Seiler, P.; Diederich, F. *Helv. Chim. Acta* **1995**, *78*, 13.
(28) Tykwinski, R. R.; Diederich, F. *Liebigs Ann./Recueil* **1997**, 649.
(29) (a) Rankin, T.; Tykwinski, R. R. *Org. Lett.* **2003**, *5*, 213. (b) Qvortrup, K.; Andersson, A. S.; Mayer, J.-P.; Jepsen, A. S.; Nielsen, M. B. *Synlett* **2004**, 2818.
(30) (a) Eisler, S.; Tykwinski, R. R. *J. Am. Chem. Soc.* **2000**, *122*, 10736. (b) Mukai, C.; Miyakoshi, N.; Hanaoka, M. *J. Org. Chem.* **2001**, *66*, 5875. (c) Eisler, S.; Chahal, N.; McDonald, R.; Tykwinski, R. R. *Chem. Eur. J.* **2003**, *9*, 2542. (d) Shi, A. L. K.; Tykwinski, R. R. *J. Org. Chem.* **2003**, *68*, 6810.
(31) Roth, W. R.; Hopf, H.; Horn, C. *Chem. Ber.* **1994**, *127*, 1781.
(32) (a) Jones, R. R.; Bergman, R. G. *J. Am. Chem. Soc.* **1972**, *94*, 660. (b) Bergman, R. G. *Acc. Chem. Res.* **1973**, *6*, 25. (c) Klein, M.; Walenzyk, T.; König, B. *Collect. Czech. Chem. Commun.* **2004**, *69*, 945. (d) Rawat, D. S.; Zaleski, J. M. *Synlett* **2004**, *3*, 393.
(33) Roth, W. R.; Hopf, H.; Horn, C. *Chem. Ber.* **1994**, *127*, 1765.
(34) Basak, A.; Mandal, S.; Bag, S. S. *Chem. Rev.* **2003**, *103*, 4077.
(35) Kaneko, T.; Takahashi, M.; Hirama, M. *Angew. Chem., Int. Ed. Engl.* **1999**, *38*, 1267.
(36) For a review on acetylenic coupling reactions, see Siemsen, P.; Livingston, R. C.; Diederich, F. *Angew. Chem., Int. Ed.* **2000**, *39*, 2632.
(37) Eglinton, G.; Galbraith, A. R. *Chem. Ind. (London)* **1956**, 737.
(38) Figeys, H. P.; Gelbcke, M. *Tetrahedron Lett.* **1970**, *11*, 5139.
(39) (a) Sonogashira, K.; Tohda, Y.; Hagihara, N. *Tetrahedron Lett.* **1975**, *16*, 4467. (b) Takahashi, S.; Kuroyama, Y.; Sonogashira, K.; Hagihara, N. *Synthesis* **1980**, 627. (c) Sonogashira, K. In *Metal-Catalyzed Cross-Coupling Reactions*; Diederich, F., Stang, P. J., Eds.; Wiley-VCH: Weinheim, 1998; pp 203−229.
(40) (a) König, B.; Schofield, E.; Bubenitschek, P.; Jones, P. G. *J. Org. Chem.* **1994**, *59*, 7142. (b) Martin, R. E.; Bartek, J.; Diederich, F.; Tykwinski, R. R.; Meister, E. C.; Hilger, A.; Lüthi, H. P. *J. Chem. Soc., Perkin Trans. 2* **1998**, 233. (c) Sakakibara, H.; Ikegami, M.; Isagawa, K.; Tojo, S.; Majima, T.; Arai, T. *Chem. Lett.* **2001**, 1050. (d) Miki, Y.; Momotake, A.; Arai, T. *Org. Biomol. Chem.* **2003**, *1*, 2655. (e) Hilger, A.; Gisselbrecht, J.-P.; Tykwinski, R. R.; Boudon, C.; Schreiber, M.; Martin, R. E.; Lüthi, H. P.; Gross, M.; Diederich, F. *J. Am. Chem. Soc.* **1997**, *119*, 2069.
(41) A 1,1-diethynylbuta-1,3-diene derivative also reacted only at the double bonds, leaving the diethynyl substitution pattern intact, according to ref 16.
(42) (a) Glaser, C. *Ber. Dtsch. Chem. Ges.* **1869**, *2*, 422. (b) Glaser, C. *Ann. Chem. Pharm.* **1870**, *154*, 137.
(43) Eshdat, L.; Berger, H.; Hopf, H.; Rabinovitz, M. *J. Am. Chem. Soc.* **2002**, *124*, 3822.
(44) Kaafarani, B. R.; Wex, B.; Bauer, J. A. K.; Neckers, D. C. *Tetrahedron Lett.* **2002**, *43*, 8227.
(45) Tinnemans, A. H. A.; Laarhoven, W. H. *Tetrahedron Lett.* **1973**, 817.
(46) Lee, M. D.; Ellestad, G. A.; Borders, D. B. *Acc. Chem. Res.* **1991**, *24*, 235.
(47) Golik, J.; Dubay, G.; Groenewold, G.; Kawaguchi, H.; Konishi, M.; Krishnan, B.; Ohkuma, H.; Doyle, T. W. *J. Am. Chem. Soc.* **1987**, *109*, 3462.
(48) (a) Goldberg, I. H. *Acc. Chem. Res.* **1991**, *24*, 191 and references therein. (b) Myers, A. G.; Proteau, P. J. *J. Am. Chem. Soc.* **1989**, *111*, 1146.
(49) Leet, J. E.; Schroeder, D. R.; Hofstead, S. J.; Golik, J.; Colson, K. L.; Huang, S.; Klohr, S. E.; Doyle, T. W. *J. Am. Chem. Soc.* **1992**, *114*, 7946.
(50) Yoshida, K.; Minami, Y.; Azuma, R.; Saeki, M.; Otani, T. *Tetrahedron Lett.* **1993**, *34*, 2637.
(51) Konishi, M.; Okhuma, H.; Tsuno, T.; Oki, T.; VanDuyne, G. D.; Clardy, J. *J. Am. Chem. Soc.* **1990**, *112*, 3715.
(52) Behr, O. M.; Eglinton, G.; Galbraith, A. R.; Raphael, R. A. *J. Chem. Soc.* **1960**, 3614.
(53) Pilling, G. M.; Sondheimer, F. *J. Am. Chem. Soc.* **1971**, *93*, 1970.
(54) Elbaum, D.; Nguyen, T. B.; Jorgensen, W. L.; Schreiber, S. L. *Tetrahedron* **1994**, *50*, 1503.
(55) For attempted reactions at the central double bond of TEE derivatives, see, for example, Lange, T.; van Loon, J.-D.; Tykwinski, R. R.; Schreiber, M.; Diederich, F. *Synthesis* **1996**, 537.
(56) Boudon, C.; Gisselbrecht, J.-P.; Gross, M.; Anthony, J.; Boldi, A. M.; Faust, R.; Lange, T.; Philp, D.; Van Loon, J.-D.; Diederich, F. *J. Electroanal. Chem.* **1995**, *394*, 187.
(57) Diederich, F. *Chem. Commun.* **2001**, 219.
(58) Hopf, H.; Kreutzer, M.; Jones, P. G. *Chem. Ber.* **1991**, *124*, 1471.
(59) Hoekstra, A.; Vos, A. *Acta Crystallogr. B* **1975**, *31*, 1716.
(60) (a) Tykwinski, R. R.; Schreiber, M.; Carlón, R. P.; Diederich, F.; Gramlich, V. *Helv. Chim. Acta* **1996**, *79*, 2249. (b) Mitzel, F.; Boudon, C.; Gisselbrecht, J.-P.; Gross, M.; Diederich, F. *Chem. Commun.* **2002**, 2318.
(61) (a) Gobbi, L.; Seiler, P.; Diederich, F. *Angew. Chem., Int. Ed.* **1999**, *38*, 674. (b) Gobbi, L.; Seiler, P.; Diederich, F.; Gramlich, V. *Helv. Chim. Acta* **2000**, *83*, 1711. (c) Gobbi, L.; Seiler, P.; Diederich, F.; Gramlich, V.; Boudon, C.; Gisselbrecht, J.-P.; Gross, M. *Helv. Chim. Acta* **2001**, *84*, 743.
(62) Gierisch, S.; Daub, J. *Chem. Ber.* **1989**, *122*, 69.
(63) Gobbi, L.; Elmaci, N.; Lüthi, H. P.; Diederich, F. *ChemPhysChem* **2001**, *2*, 423.
(64) (a) Rotkiewicz, K.; Grellmann, K. H.; Grabowski, Z. R. *Chem. Phys. Lett.* **1973**, *19*, 315. (b) Rotkiewicz, K.; Grabowski, Z. R.; Krówczyñski, A.; Kühnle, W. *J. Lumin.* **1976**, *12/13*, 877. (c) Grabowski, Z. R.; Rotkiewicz, K.; Siemiarczuk, A. *J. Lumin.* **1979**, *18/19*, 420. (d) Grabowski, Z. R.; Rotkiewicz, K.; Siemiarczuk, A.; Cowley, D. J.; Baumann, W. *Nouv. J. Chim.* **1979**, *3*, 443.
(65) Martin, R. E.; Gubler, U.; Boudon, C.; Gramlich, V.; Bosshard, C.; Gisselbrecht, J.-P.; Günter, P.; Gross, M.; Diederich, F. *Chem. Eur. J.* **1997**, *3*, 1505.
(66) Zhao, Y.; Campbell, K.; Tykwinski, R. R. *J. Org. Chem.* **2002**, *67*, 336.
(67) Bruschi, M.; Giuffreda, M. G.; Lüthi, H. P. *Chem. Eur. J.* **2002**, *8*, 4216.
(68) Perichon, J.; Herlem, M.; Bobilliart, F.; Thiebault, A.; Nyberg, K. In *Encyclopedia of Electrochemistry of the Elements—Organic Section*; Bard, A. J., Lund, H., Eds.; Dekker: New York, 1978; Vol. 11, Chapter 1.
(69) For a recent microreview on the redox properties of linear and cyclic DEE and TEE scaffolds, see Gisselbrecht, J.-P.; Moonen, N. N. P.; Boudon, C.; Nielsen, M. B.; Diederich, F.; Gross, M. *Eur. J. Org. Chem.* **2004**, 2959.
(70) For X-ray crystal structures, see, for example, (a) refs 27b, 58, 60a, 65, and 66. (b) Diederich, F.; Philp, D.; Seiler, P. *J. Chem. Soc., Chem. Commun.* **1994**, 205. (c) Taniguchi, H.; Hayashi, K.; Nishioka, K.; Hori, Y.; Shiro, M.; Kitamura, T. *Chem. Lett.* **1994**, 1921. (d) Philp, D.; Gramlich, V.; Seiler, P.; Diederich, F. *J. Chem. Soc., Perkin Trans 2* **1995**, 875. (e) Nikas, S.; Rodios, N. A.; Varvoglis, A.; Terzis, A.; Raptopoulou, C. P. *J. Heterocycl. Chem.* **1996**, *33*, 997. (f) Nierengarten, J.-F.; Schreiber, M.; Diederich, F.; Gramlich, V. *New J. Chem.* **1996**, *20*, 1273. (g) Tykwinski, R. R.; Schreiber, M.; Gramlich, V.; Seiler, P.; Diederich, F. *Adv. Mater.* **1996**, *8*, 226. (h) Tykwinski, R. R.; Hilger, A.; Diederich, F.; Lüthi, H. P.; Seiler, P.; Gramlich, V.; Gisselbrecht, J.-P.; Boudon, C.; Gross, M. *Helv. Chim. Acta* **2000**, *83*, 1484.
(71) For early ab initio calculations on TEE structures, see (a) Ma, B.; Xie, Y.; Schaefer, H. F. *Chem. Phys. Lett.* **1992**, *191*, 521. (b) Ma, B.; Sulzbach, H. M.; Xie, Y.; Schaefer, H. F. *J. Am. Chem. Soc.* **1994**, *116*, 3529.
(72) Ciulei, S. C.; Tykwinski, R. R. *Org. Lett.* **2000**, *2*, 3607.
(73) Zhao, Y.; Ciulei, S. C.; Tykwinski, R. R. *Tetrahedron Lett.* **2001**, *42*, 7721.
(74) Dehu, C.; Meyers, F.; Brédas, J. L. *J. Am. Chem. Soc.* **1993**, *115*, 6198.
(75) (a) Bosshard, C.; Spreiter, R.; Günter, P.; Tykwinski, R. R.; Schreiber, M.; Diederich, F. *Adv. Mater.* **1996**, *8*, 231. (b) Spreiter, R.; Bosshard, C.; Knöpfle, G.; Günter, P.; Tykwinski, R. R.; Schreiber, M.; Diederich, F. *J. Phys. Chem. B* **1998**, *102*, 29. (c) Tykwinski, R. R.; Gubler, U.; Martin, R. E.; Diederich, F.; Bosshard, C.; Günter, P. *J. Phys. Chem. B* **1998**, *102*, 4451. (d) Gubler, U.; Spreiter, R.; Bosshard, C.; Günter, P.; Tykwinski, R. R.; Diederich, F. *Appl. Phys. Lett.* **1998**, *73*, 2396. (e) Bosshard, C. In *Nonlinear Optical Effects and Materials*; Günter, P., Ed.; Springer-Verlag: Berlin, 2000; pp 7−161.
(76) The extensive studies on TEE derivatives have revealed that both acentricity and donor/acceptor strength influence the third-order nonlinear optical properties; see ref 75.
(77) McQuilkin, R. M.; Garratt, P. J.; Sondheimer, F. *J. Am. Chem. Soc.* **1970**, *92*, 6682.
(78) Burri, E.; Diederich, F.; Nielsen, M. B. *Helv. Chim. Acta* **2001**, *85*, 2169.
(79) Zhao, Y.; McDonald, R.; Tykwinski, R. R. *J. Org. Chem.* **2002**, *67*, 2805.
(80) Boldi, A. M.; Anthony, J.; Gramlich, V.; Knobler, C. B.; Boudon, C.; Gisselbrecht, J.-P.; Gross, M.; Diederich, F. *Helv. Chim. Acta* **1995**, *78*, 779.
(81) Nielsen, M. B.; Schreiber, M.; Baek, Y. G.; Seiler, P.; Lecomte, S.; Boudon, C.; Tykwinski, R. R.; Gisselbrecht, J.-P.; Gramlich, V.; Skinner, P. J.; Bosshard, C.; Günter, P.; Gross, M.; Diederich, F. *Chem. Eur. J.* **2001**, *7*, 3263.
(82) (a) Metler, T.; Uchida, A.; Miller, S. I. *Tetrahedron* **1968**, *24*, 4285. (b) Ukhin, L. Y.; Sladkov, A. M.; Orlova, Z. I. *Bull. Acad. Sci. USSR, Div. Chem. Sci.* **1969**, 637. (c) Dulog, L.; Körner, B.; Heinze, J.; Yang, J. J. *Liebigs Ann.* **1995**, 1663. (d) Hopf, H.; Kreutzer, M. *Angew. Chem., Int. Ed. Engl.* **1990**, *29*, 393. (e)

Moonen, N. N. P.; Boudon, C.; Gisselbrecht, J.-P.; Seiler, P.; Gross, M.; Diederich, F. *Angew. Chem., Int. Ed.* **2002**, *41*, 3044. (f) Moonen, N. N. P.; Gist, R.; Boudon, C.; Gisselbrecht, J.-P.; Seiler, P.; Kawai, T.; Kishioka, A.; Gross, M.; Irie, M.; Diederich, F. *Org. Biomol. Chem.* **2003**, *1*, 2032. (g) Moonen, N. N. P.; Diederich, F. *Org. Biomol. Chem.* **2004**, *2*, 2263.

(83) Diaz, C.; Arancibia, A. *Polyhedron* **2000**, *19*, 137.

(84) (a) Seitz, G.; Sutrisno, R.; Gerecht, B.; Offermann, G.; Schmidt, R.; Massa, W. *Angew. Chem., Int. Ed. Engl.* **1982**, *21*, 283. (b) Blinka, T. A.; West, R. *Tetrahedron Lett.* **1983**, *24*, 1567.

(85) Hopf, H.; Kämpen, J.; Bubenitschek, P.; Jones, P. G. *Eur. J. Org. Chem.* **2002**, 1708.

(86) Neidlein, R.; Winter, M. *Synthesis* **1998**, 1362.

(87) Skattebøl, L.; Charlton, J. L.; deMayo, P. *Tetrahedron Lett.* **1966**, *7*, 2257.

(88) (a) *Handbook of Conducting Polymers, Second Edition, Revised and Expanded*; Skotheim, T. A., Elsenbaumer, R. L., Reynolds, J. R., Eds.; Marcel Dekker: New York, 1998. (b) McQuade, D. T.; Pullen, A. E.; Swager, T. M. *Chem. Rev.* **2000**, *100*, 2537. (c) Bunz, U. H. F. *Chem. Rev.* **2000**, *100*, 1605.

(89) (a) Chiang, C. K.; Fincher, C. R., Jr.; Park, Y. W.; Heeger, A. J.; Shirakawa, H.; Louis, E. J.; Gau, S. C.; MacDiarmid, A. G. *Phys. Rev. Lett*. **1977**, *39*, 1098. (b) Shirakawa, H. *Angew. Chem., Int. Ed.* **2001**, *40*, 2574. (c) MacDiarmid, A. G. *Angew. Chem., Int. Ed.* **2001**, *40*, 2581. (d) Heeger, A. J. *Angew. Chem., Int. Ed.* **2001**, *40*, 2591.

(90) (a) Müllen, K. *Pure Appl. Chem.* **1993**, *65*, 89. (b) Tour, J. M. *Chem. Rev.* **1996**, *96*, 537. (c) Wegner, G.; Müllen, K. *Electronic Materials—The Oligomer Approach*; Wiley-VCH: Weinheim, 1998. (d) Martin, R. E.; Diederich, F. *Angew. Chem., Int. Ed.* **1999**, *38*, 1350.

(91) Kubatkin, S.; Danilov, A.; Hjort, M.; Cornil, J.; Brédas, J.-L.; Stuhr-Hansen, N.; Hedegård, P.; Bjørnholm, T. *Nature* **2003**, *425*, 698.

(92) (a) Wenz, G.; Müller, M. A.; Schmidt, M.; Wegner, G. *Macromolecules* **1984**, *17*, 837. (b) Wudl, F.; Bitler, S. P. *J. Am. Chem. Soc.* **1986**, *108*, 4685. (c) Giesa, R.; Schulz, R. C. *Polym. Int.* **1994**, *33*, 43.

(93) Lindsell, W. E.; Preston, P. N.; Tomb, P. J. *J. Organomet. Chem.* **1992**, *439*, 201.

(94) Bharucha, K. N.; Marsh, R. M.; Minto, R. E.; Bergman, R. G. *J. Am. Chem. Soc.* **1992**, *114*, 3120.

(95) Kosinski, C.; Hirsch, A.; Heinemann, F. W.; Hampel, F. *Eur. J. Org. Chem.* **2001**, 3879.

(96) (a) Anthony, J.; Boudon, C.; Diederich, F.; Gisselbrecht, J.-P.; Gramlich, V.; Gross, M.; Hobi, M.; Seiler, P. *Angew. Chem., Int. Ed. Engl.* **1994**, *33*, 763. (b) Schreiber, M.; Tykwinski, R. R.; Diederich, F.; Spreiter, R.; Gubler, U.; Bosshard, C.; Poberaj, I.; Günter, P.; Boudon, C.; Gisselbrecht, J.-P.; Gross, M.; Jonas, U.; Ringsdorf, H. *Adv. Mater.* **1997**, *9*, 339. (c) Schenning, A. P. H. J.; Martin, R. E.; Ito, M.; Diederich, F.; Boudon, C.; Gisselbrecht, J.-P.; Gross, M. *Chem. Commun.* **1998**, 1013. (d) Martin, R. E.; Gubler, U.; Boudon, C.; Bosshard, C.; Gisselbrecht, J.-P.; Günter, P.; Gross, M.; Diederich, F. *Chem. Eur. J.* **2000**, *6*, 4400. (e) Xiao, J.; Yang, M.; Lauher, J. W.; Fowler, F. W. *Angew. Chem., Int. Ed.* **2000**, *39*, 2132. (f) Martin, R. E.; Gubler, U.; Cornil, J.; Balakina, M.; Boudon, C.; Bosshard, C.; Gisselbrecht, J.-P.; Diederich, F.; Günter, P.; Gross, M.; Brédas, J.-L. *Chem. Eur. J.* **2000**, *6*, 3622. (g) Schenning, A. P. H. J.; Arndt, J.-D.; Ito, M.; Stoddart, A.; Schreiber, M.; Siemsen, P.; Martin, R. E.; Boudon, C.; Gisselbrecht, J.-P.; Gross, M.; Gramlich, V.; Diederich, F. *Helv. Chim. Acta* **2001**, *84*, 296. (h) Edelmann, M. J.; Estermann, M. A.; Gramlich, V.; Diederich, F. *Helv. Chim. Acta* **2001**, *84*, 473. (i) Nierengarten, J.-F. *Helv. Chim. Acta* **2004**, *87*, 1357.

(97) Rissler, J. *Chem. Phys. Lett.* **2004**, *395*, 92.

(98) (a) Bailey, W. J.; Nielsen, N. A. *J. Org. Chem.* **1962**, *27*, 3088. (b) Hopf, H. *Angew. Chem., Int. Ed. Engl.* **1984**, *23*, 948. (c) Fielder, S.; Rowan, D. D.; Sherburn, M. S. *Angew. Chem., Int. Ed.* **2000**, *39*, 4331.

(99) For an account of cross-conjugated oligo(enynes), see Tykwinski, R. R.; Zhao, Y. *Synlett* **2002**, 1939.

(100) Zhao, Y.; McDonald, R.; Tykwinski, R. R. *Chem. Commun.* **2000**, 77.

(101) For each of **131b**−**i**, the longest wavelength absorption band is very broad. For this reason, the energy corresponding to the wavelength at which the extinction coefficient is half its maximum value at the lower energy tail of the absorption band is plotted. See ref 66.

(102) For NLO characteristics of *iso*-PDAs, see (a) Slepkov, A. D.; Hegmann, F. A.; Zhao, Y.; Tykwinski, R. R.; Kamada, K. *J. Chem. Phys.* **2002**, *116*, 3834. (b) Slepkov, A. D.; Hegmann, F. A.; Kamada, K.; Zhao, Y.; Tykwinski, R. R. *J. Opt. A.: Pure Appl. Opt.* **2002**, *4*, S207. (c) Ref 19b.

(103) (a) Wytko, J.; Berl, V.; McLaughlin, M.; Tykwinski, R. R.; Schreiber, M.; Diederich, F.; Boudon, C.; Gisselbrecht, J.-P.; Gross, M. *Helv. Chim. Acta* **1998**, *81*, 1964. (b) Maya, E. M.; Vazquez, P.; Torres, T.; Gobbi, L.; Diederich, F.; Pyo, S.; Echegoyen, L. *J. Org. Chem.* **2000**, *65*, 823. (c) Martin, R. E.; Wytko, J. A.; Diederich, F.; Boudon, C.; Gisselbrecht, J.-P.; Gross, M. *Helv. Chim. Acta* **1999**, *82*, 1470. (d) Edelmann, M. J.; Odermatt, S.; Diederich, F. *Chimia* **2001**, *55*, 132. (e) Edelmann, M. J.; Raimundo, J.-M.; Utesch, N. F.; Diederich, F.; Boudon, C.; Gisselbrecht, J.-P.; Gross, M. *Helv. Chim. Acta* **2002**, *85*, 2195. (f) Utesch, N. F.; Diederich, F. *Org. Biomol. Chem.* **2003**, *1*, 237. (g) Nakano, Y.; Ishizuka, K.; Muraoka, K.; Ohtani, H.; Takayama, Y.; Sato, F. *Org. Lett.* **2004**, *6*, 2373.

(104) For NLO studies on in-backbone substituted PTAs, see (a) Gubler, U.; Concilio, S.; Bosshard, C.; Biaggio, I.; Günter, P.; Martin, R. E.; Edelmann, M.; Wytko, J.; Diederich, F. *Appl. Phys. Lett.* **2002**, *81*, 2322. (b) Concilio, S.; Biaggio, I.; Günter, P.; Piotto, S.; Edelman, M.; Raimundo, J.-M.; Diederich, F. *J. Opt. Soc. Am. B* **2003**, *20*, 1656.

(105) (a) Scherf, U.; Müllen, K. *Synthesis* **1992**, 23. (b) Garay, R. O.; Naarmann, H.; Müllen, K. *Macromolecules* **1994**, *27*, 1922.

(106) Taylor, P. N.; Wylie, A. P.; Huuskonen, J.; Anderson, H. L. *Angew. Chem., Int. Ed. Engl.* **1998**, *37*, 986.

(107) (a) Diederich, F.; Faust, R.; Gramlich, V.; Seiler, P. *J. Chem. Soc., Chem. Commun.* **1994**, 2045. (b) Faust, R.; Diederich, F.; Gramlich, V.; Seiler, P. *Chem. Eur. J.* **1995**, *1*, 111. (c) Siemsen, P.; Gubler, U.; Bosshard, C.; Günter, P.; Diederich, F. *Chem. Eur. J.* **2001**, *7*, 1333.

(108) For other metal−acetylide complexes based on DEEs and TEEs, see (a) Lu, W.; Zhu, N.; Che, C.-M. *J. Organomet. Chem.* **2003**, *670*, 11. (b) Campbell, K.; McDonald R.; Ferguson, M. J.; Tykwinski, R. R. *Organometallics* **2003**, *22*, 1353. (c) Shi, Y.; Yee, G. T.; Wang, G.; Ren, T. *J. Am. Chem. Soc.* **2004**, *126*, 10552.

(109) (a) Shultz, D. A.; Lee, H.; Gwaltney, K. P. *J. Org. Chem.* **1998**, *63*, 7584. (b) Shultz, D. A.; Lee, H.; Kumar, R. K.; Gwaltney, K. P. *J. Org. Chem.* **1999**, *64*, 9124.

(110) (a) Nielsen, M. B.; Lomholt, C.; Becher, J. *Chem. Soc. Rev.* **2000**, *29*, 153. (b) Bryce, M. R. *J. Mater. Chem.* **2000**, *10*, 589. (c) Segura, J. L.; Martín, N. *Angew. Chem., Int. Ed.* **2001**, *40*, 1372.

(111) Williams, J. M.; Ferraro, J. R.; Thorn, R. J.; Carlson, K. D.; Geiser, U.; Wang, H. H.; Kini, A. M.; Whangbo, M.-H. *Organic Superconductors (Including Fullerenes): Synthesis, Structure, Properties, and Theory*; Prentice Hall: Englewood Cliffs, New Jersey, 1992.

(112) Luo, Y.; Collier, C. P.; Jeppesen, J. O.; Nielsen, K. A.; Delonno, E.; Ho, G.; Perkins, J.; Tseng, H.-R.; Yamamoto, T.; Stoddart, J. F.; Heath, J. R. *ChemPhysChem* **2002**, *3*, 519.

(113) Roncali, J. *J. Mater. Chem.* **1997**, *7*, 2307.

(114) Nielsen. M. B.; Utesch, N. F.; Moonen, N. N. P.; Boudon, C.; Gisselbrecht, J.-P.; Concilio, S.; Piotto, S. P.; Seiler, P.; Günter, P.; Gross, M.; Diederich, F. *Chem. Eur. J.* **2002**, *8*, 3601.

(115) Nielsen, M. B.; Gisselbrecht, J.-P.; Thorup, N.; Piotto, S. P.; Boudon, C.; Gross, M. *Tetrahedron Lett.* **2003**, *44*, 6721.

(116) For examples of diacetylenic dithiafulvenes containing the *gem*-DEE structural motif, see (a) Ref 114. (b) Kumagai, T.; Tomura, M.; Nishida, J.; Yamashita, Y. *Tetrahedron Lett.* **2003**, *44*, 6845.

(117) Nguyen, T.-T.; Gouriou, Y.; Sallé, M.; Frère, P.; Jubault, M.; Gorgues, A.; Toupet, L.; Riou, A. *Bull. Soc. Chim. Fr.* **1996**, *133*, 301.

(118) (a) Hwang, G. T.; Son, H. S.; Ku, J. K.; Kim, B. H. *Org. Lett.* **2001**, *3*, 2469. (b) Hwang, G. T.; Son, H. S.; Ku, J. K.; Kim, B. H. *J. Am. Chem. Soc.* **2003**, *125*, 11241.

(119) Hwang, G. T.; Kim, B. H. *Org. Lett.* **2004**, *6*, 2669.

(120) Kaafarani, B. R.; Wex, B.; Wang, F.; Catanescu, O.; Chien, L. C.; Neckers, D. C. *J. Org. Chem.* **2003**, *68*, 5377.

(121) Ito, S.; Inabe, H.; Morita, N.; Tajiri, A. *Eur. J. Org. Chem.* **2004**, 1774.

(122) (a) Sondheimer, F.; Wolovsky, R. *Tetrahedron Lett.* **1959**, *3*, 3. (b) Sondheimer, F.; Wolovsky, R.; Amiel, Y. *J. Am. Chem. Soc.* **1962**, *84*, 274.

(123) (a) Wolovsky, R.; Sondheimer, F. *J. Am. Chem. Soc.* **1965**, *87*, 5720. (b) Sondheimer, F.; Wolovsky, R.; Garratt, P. J.; Calder, I. C. *J. Am. Chem. Soc.* **1966**, *88*, 2610. (c) Untch, K. G.; Wysocki, D. C. *J. Am. Chem. Soc.* **1966**, *88*, 2608. (d) Untch, K. G.; Wysocki, D. C. *J. Am. Chem. Soc.* **1967**, *89*, 6386.

(124) Diederich, F.; Rubin, Y.; Knobler, C. B.; Whetten, R. L.; Schriver, K. E.; Houk, K. N.; Li, Y. *Science* **1989**, *245*, 1088.

(125) (a) Rubin, Y.; Diederich, F. *J. Am. Chem. Soc.* **1989**, *111*, 6870. (b) Li, Y.; Rubin, Y.; Diederich, F.; Houk, K. N. *J. Am. Chem. Soc.* **1990**, *112*, 1618. (c) Rubin, Y.; Kahr, M.; Knobler, C. B.; Diederich, F.; Wilkins, C. L. *J. Am. Chem. Soc.* **1991**, *113*, 495. (d) Diederich, F.; Rubin, Y.; Chapman, O. L.; Goroff, N. S. *Helv. Chim. Acta* **1994**, *77*, 1441.

(126) (a) Anthony, J.; Knobler, C. B.; Diederich, F. *Angew. Chem., Int. Ed. Engl.* **1993**, *32*, 406. (b) Anthony, J.; Boldi, A. M.; Boudon, C.; Gisselbrecht, J.-P.; Gross, M.; Seiler, P.; Knobler, C. B.; Diederich, F. *Helv. Chim. Acta* **1995**, *78*, 797.

(127) (a) Mitzel, F.; Boudon, C.; Gisselbrecht, J.-P.; Seiler, P.; Gross, M.; Diederich, F. *Chem. Commun.* **2003**, 1634. (b) Mitzel, F.; Boudon, C.; Gisselbrecht, J.-P.; Seiler, P.; Gross, M.; Diederich, F. *Helv. Chim. Acta* **2004**, *87*, 1130.

(128) For a review on radialenes, see Hopf, H.; Maas, G. *Angew. Chem., Int. Ed. Engl.* **1992**, *31*, 931.

(129) Lange, T.; Gramlich, V.; Amrein, W.; Diederich, F.; Gross, M.; Boudon, C.; Gisselbrecht, J.-P. *Angew. Chem., Int. Ed. Engl.* **1995**, *34*, 805.
(130) Lepetit, C.; Nielsen, M. B.; Diederich, F.; Chauvin, R. *Chem. Eur. J.* **2003**, *9*, 5056.
(131) (a) Eisler, S.; Tykwinski, R. R. *Angew. Chem., Int. Ed. Engl.* **1999**, *38*, 1940. (b) Eisler, S.; McDonald, R.; Loppnow, G. R.; Tykwinski, R. R. *J. Am. Chem. Soc.* **2000**, *122*, 6917.
(132) Tobe, T.; Umeda, R.; Iwasa, N.; Sonoda, M. *Chem. Eur. J.* **2003**, *9*, 5549.
(133) For the formation of linear polyynes from acyclic *gem*-DEE analogues of **209**, see Tobe, Y.; Iwasa, N.; Umeda, R.; Sonoda, M. *Tetrahedron Lett.* **2001**, *42*, 5485.
(134) Echegoyen, L.; Diederich, F.; Echegoyen, L. Electrochemistry of fullerenes. In *Fullerenes: Chemistry, Physics and Technology*; Kadish, K. D., Ruoff, R. S., Eds.; Wiley-VCH: New York, 2000; pp 1−51.
(135) (a) Staab, H. A.; Bader, R. *Chem. Ber.* **1970**, *103*, 1157. (b) Staab, H. A.; Graf, F. *Chem. Ber.* **1970**, *103*, 1107. (c) Meissner, U.; Meissner, B.; Staab, H. A. *Angew. Chem., Int. Ed. Engl.* **1973**, *12*, 916. (d) Yasuhara, A.; Satake, T.; Iyoda, M.; Nakagava, M. *Tetrahedron Lett.* **1975**, *16*, 895. (e) Meissner, U. E.; Gensler, A.; Staab, H. A. *Angew. Chem., Int. Ed. Engl.* **1976**, *15*, 365. (f) Darby, N.; Cresp, T. M.; Sondheimer, F. *J. Org. Chem.* **1977**, *42*, 1960. (g) Sakano, K.; Akiyama, S.; Iyoda, M.; Nakagawa, M. *Chem. Lett.* **1978**, 1023. (h) Wan, W. B.; Kimball, D. B.; Haley, M. M. *Tetrahedron Lett.* **1998**, *39*, 6795. (i) Matzger, A. J.; Vollhardt, K. P. C. *Tetrahedron Lett.* **1998**, *39*, 6791. (j) Bell, M. L.; Chiechi, R. C.; Johnson, C. A.; Kimball, D. B.; Matzger, A. J.; Wan, W. B.; Weakley, T. J. R.; Haley, M. M. *Tetrahedron* **2001**, *57*, 3507. (k) Wan, W. B.; Chiechi, R. C.; Weakley, T. J. R.; Haley, M. M. *Eur. J. Org. Chem.* **2001**, 3485. (l) Jusélius, J.; Sundholm, D. *Phys. Chem. Chem. Phys.* **2001**, *3*, 2433.
(136) (a) Boydston, A. J.; Haley, M. M. *Org. Lett.* **2001**, *3*, 3599. (b) Boydston, A. J.; Haley, M. M.; Williams, R. V.; Armantrout, J. R. *J. Org. Chem.* **2002**, *67*, 8812.
(137) (a) Blanchette, H. S.; Brand, S. C.; Naruse, H.; Weakley, T. J. R.; Haley, M. M. *Tetrahedron* **2000**, *56*, 9581. (b) Baldwin, K. P.; Matzger, A. J.; Scheiman, D. A.; Tessier, C. A.; Vollhardt, K. P. C.; Youngs, W. J. *Synlett* **1995**, 1215.
(138) (a) Laskoski, M.; Steffen, W.; Smith, M. D.; Bunz, U. H. F. *Chem. Commun.* **2001**, 691. (b) Laskoski, M.; Smith, M. D.; Morton, J. G. M.; Bunz, U. H. F. *J. Org. Chem.* **2001**, *66*, 5174. (c) Laskoski, M.; Steffen, W.; Morton, J. G. M.; Smith, M. D.; Bunz, U. H. F. *J. Am. Chem. Soc.* **2002**, *124*, 13814.
(139) Srinivasan, M.; Sankararaman, S.; Dix, I.; Jones, P. G. *Org. Lett.* **2000**, *2*, 3849.
(140) Boydston, A. J.; Bondarenko, L.; Dix, I.; Weakley, T. J. R.; Hopf, H.; Haley, M. M. *Angew. Chem., Int. Ed.* **2001**, *40*, 2986.
(141) Rubin, Y. *Chem. Eur. J.* **1997**, *3*, 1009.
(142) (a) Rubin, Y.; Parker, T. C.; Pastor, S. J.; Jalisatgi, S.; Boulle, C.; Wilkins, C. L. *Angew. Chem., Int. Ed. Engl.* **1998**, *37*, 1226. (b) Tobe, Y.; Nakagawa, N.; Naemura, K.; Wakabayashi, T.; Shida, T.; Achiba, Y. *J. Am. Chem. Soc.* **1998**, *120*, 4544. (c) Tobe, Y.; Nakagawa, N.; Kishi, J.; Sonoda, M.; Naemura, K.; Wakabayashi, T.; Shida, T.; Achiba, Y. *Tetrahedron* **2001**, *57*, 3629.
(143) (a) Diederich, F.; Rubin, Y. *Angew. Chem., Int. Ed. Engl.* **1992**, *31*, 1101. (b) Goroff, N. S. *Acc. Chem. Res.* **1996**, *29*, 77.
(144) Rubin, Y.; Parker, T. C.; Khan, S. I.; Holliman, C. L.; McElvany, S. W. *J. Am. Chem. Soc.* **1996**, *118*, 5308.
(145) Zimmermann, G.; Nuechter, U.; Hagen, S.; Nuechter, M. *Tetrahedron Lett.* **1994**, *35*, 4747.
(146) König, B.; Rütters, H. *Tetrahedron Lett.* **1994**, *35*, 3501.
(147) For reviews or recent papers on changing the reactivity of DEEs by metal ion coordination or H-bonding, see (a) König, B. *Eur. J. Org. Chem.* **2000**, 381. (b) Ref 34. (c) Basak, A.; Bag, S. S.; Bdour, H. M. M. *Chem. Commun.* **2003**, 2614.
(148) (a) Campbell, K.; Tiemstra, N. M.; Prepas-Strobeck, N. S.; McDonald, R.; Ferguson, M. J.; Tykwinski, R. R. *Synlett* **2004**, 182. (b) Campbell, K.; Kuehl, C. J.; Ferguson, M. J.; Stang, P. J.; Tykwinski, R. R. *J. Am. Chem. Soc.* **2002**, *124*, 7266.
(149) Behr, O. M.; Eglinton, G.; Galbraith, A. R.; Raphael, R. A. *J. Chem. Soc.* **1960**, 3614.
(150) Hay, A. S. *J. Org. Chem.* **1960**, *25*, 1275.

CR9903353